

SPACE COMMUNICATIONS AND NAVIGATION PROGRAM

CoSMOS

Commercial Systems for Mission Operations Suitability

Algorithm Description Document

October 2021



National Aeronautics and
Space Administration

NASA Headquarters
Washington, D.C.

Table of Contents

1	INTRODUCTION	1-1
1.1	Scope and Purpose	1-2
1.2	ADD Structure	1-2
2	DOCUMENT TREE AND REFERENCES	2-2
2.1	Document Tree.....	2-2
2.2	References.....	2-3
3	COSMOS CALCULATIONS AND ALGORITHMS	3-4
3.1	Coverage Computations and Algorithms	3-5
3.1.1	Coverage	3-5
3.1.2	Coverage Gap Metrics	3-8
3.2	RF POWER.....	3-9
3.2.1	Minimum EIRP Calculation	3-10
3.2.1.1	DTE Minimum EIRP Calculations	3-10
3.2.1.2	Regenerative Transponder Minimum EIRP Calculation	3-12
3.2.1.3	Bent-Pipe Transponder Minimum EIRP Calculation	3-12
3.2.2	Modulation and Coding Optimization	3-13
3.3	Effective Communications Time/Throughput	3-14
3.3.1	Effective Communications Time	3-14
3.3.2	Throughput.....	3-16
3.4	User Burden	3-17
3.4.1	Antenna Size and Weight Calculations.....	3-17
3.4.1.1	Parabolic size and weight.....	3-18
3.4.1.2	Helix antenna size and weight	3-19
3.4.1.3	Electronically steerable antenna size and weight.....	3-19
3.4.1.4	Patch Antenna size and Gain	3-19
3.4.1.5	Dipole Antenna size and Gain	3-20
3.4.2	Antenna Pointing Requirements / Limitations.....	3-20
3.4.3	Pointing Reduced Coverage.....	3-22
3.5	Data Analytics.....	3-24
3.6	System Performance Comparison	3-26
	Acronyms.....	1
	Generalized Additive Model Regressions	1
	Model Descriptions.....	1
	B.1.1 Model Description: Relay Systems	1
	B.1.2 Model Description: DTE Systems.....	2

B.1.3	Model Verification.....	3
B.1.4	IridiumNext Coverage Results.....	3
B.1.5	IridiumNext MEAN Contacts per Orbit Results.....	5

List of Figures

Figure 1-1: CoSMOS Overview	1-1
Figure 2-1: CoSMOS Documentation.....	2-3
Figure 3-1: Depiction of CoSMOS Interconnectivity.....	3-5
Figure 3-2: Illustration of Latency Contributions	3-8
Figure 3-3: Modeling and Relationships between Technical Performance Evaluation Components.....	3-15
Figure 3-4: Logic Flow: Reference Antenna Size and Mass	3-17
Figure 3-5: COTS pointing rate feasibility assessment algorithm	3-22
Figure 3-6: Logic Flow: Analyze / System Comparison Ranking.....	3-27
Figure B-1. GAM regression of IridiumNext Coverage dataset with raw data points.....	4
Figure B-2. Evaluation plots for the IridiumNext Coverage regression.	5
Figure B-3. GAM regression of IridiumNext Mean Contacts per Orbit Dataset with Raw Data Points.	6
Figure B-4. Evaluation plots for the IridiumNext Coverage regression.	7
Figure B-5. GAM regression of OneWebMEO Mean Contacts per Orbit dataset with raw data points.	8
Figure B-6. Evaluation plots for the IridiumNext Coverage regression.	9
Figure B-7. GAM regression for visibility-based coverage for a generic Panama-based ground station location over 30 days	10
Figure B-8. Distribution of errors between regression prediction values and simulation provided dataset.	11
Figure B-9. GAM regression for visibility-based coverage for a generic Svalbard-based ground station location over 30 days.	12
Figure B-10. Distribution of errors between regression prediction values and simulation provided dataset at dataset values greater than 0.	13
Figure B-11. Distribution of errors between regression prediction values and simulation provided dataset at dataset values equal to 0.	13
Figure B-12. GAM regression for visibility based coverage for a summation of generic Svalbard-based and Santiago-based ground station location coverages over 30 days.	14
Figure B-13. Distribution of errors between regression prediction values and simulation provided dataset at dataset values greater than 0.	15
Figure B-14. Distribution of errors between regression prediction values and simulation provided dataset at dataset values equal to 0.	15
Figure B-15. GAM regression for visibility-based coverage for a summation of generic Svalbard, Santiago, and Panama based ground station location coverages over 30 days.....	16
Figure B-16. Distribution of errors between regression prediction values and simulation provided dataset.	17

List of Tables

Table 3-1: Coverage Computations and Algorithms Inputs & Outputs.....	3-6
Table 3-2: Coverage Gap Metrics Computations and Algorithm Inputs and Outputs.....	3-9

Table 3-3: DTE Link Budget	3-11
Table 3-4: Coding and Modulation Optimization Algorithm Inputs and Outputs	3-14
Table 3-5: Effective Communications Time Inputs and Outputs	3-15
Table 3-6: Throughput Calculations Inputs and Outputs	3-16
Table 3-7: User Burden Computations & Algorithms Inputs and Outputs.....	3-18
Table 3-8: Sample Antenna Pointing Mechanisms from Moog Inc.	3-22
Table 3-9: Pointing Reduced Coverage Calculations & Algorithms Inputs and Outputs.....	3-23
Table 3-10: Analytics Computations and Algorithms Inputs and Outputs	3-26
Table 3-11: System Performance Algorithm Inputs and Outputs	3-27

1 INTRODUCTION

The Space Communications and Navigation (SCaN) Program at NASA is moving toward further commercialization of communications and navigation services for NASA user missions in near-Earth space. The Commercial Systems for Mission Operations Suitability (CoSMOS) platform is intended to assist in this transition by providing a user-friendly means of evaluating how well a specific commercial system will support a given NASA user's communication needs.

CoSMOS uses results from previous simulation runs to estimate the performance and applicability of a communication system by using a combination of statistical techniques and traditional communication systems computation techniques and algorithms.

CoSMOS can be used to rapidly assess the suitability of both Commercial and NASA networks to meet a specific user mission's communications need. Users of CoSMOS may include SCaN systems engineers or engineers supporting engagement with missions early in their planning and design lifecycle.

As show in in Figure 1-1, CoSMOS supports an evaluation workflow that starts with mission requirements such as orbit, throughput requirements, latency needs, and launch year. Using its statistical and analysis engine, CoSMOS generates communication metrics such as coverage percentage, average coverage gap duration and user minimum EIRP for the specified mission.

This Algorithm Description Document (ADD) details the data calculations, algorithms regression modeling functions embedded in CoSMOS statistical and analyses engine, and the analyzer and comparison tools.

This ADD will be updated appropriately as CoSMOS evolves.

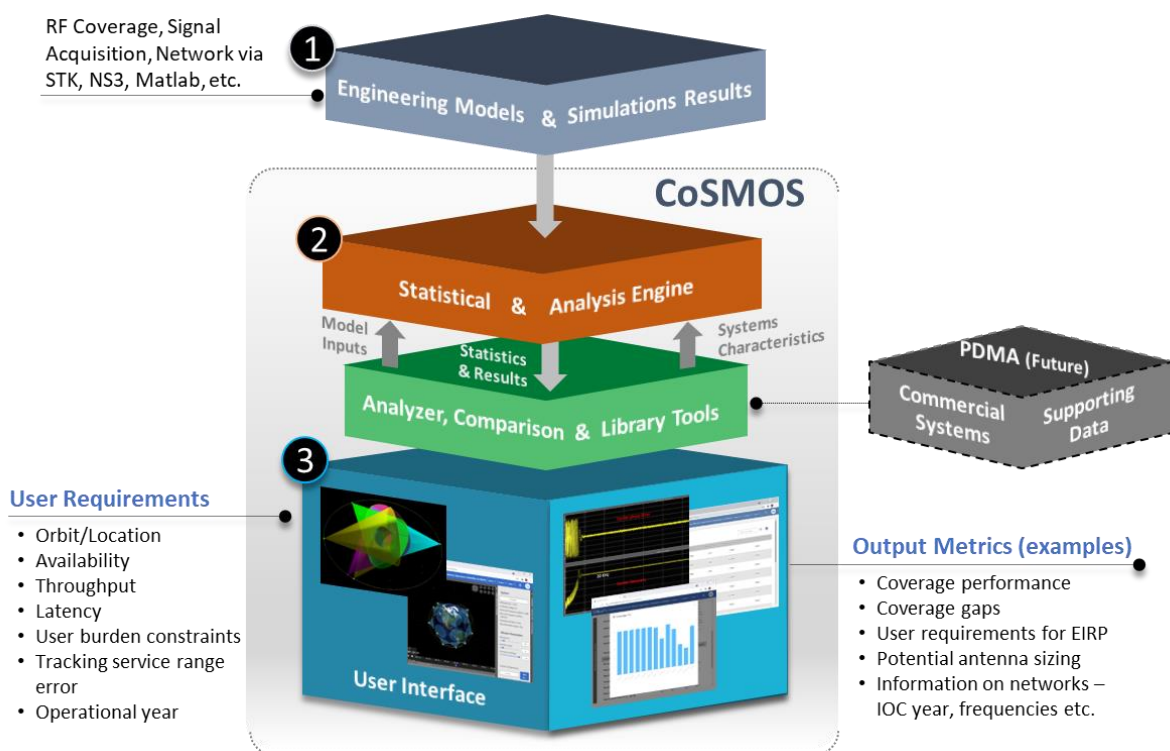


Figure 1-1: CoSMOS Overview

1.1 Scope and Purpose

This ADD is intended to provide the CoSMOS user with the details of the statistical and mathematical computations and algorithms performed to derive the predicted performance metrics. It provides a detailed description of the analytical processes embedded in CoSMOS to allow users to understand how results are generated, capabilities, and limitations.

1.2 ADD Structure

This ADD is structured as follows:

- 1) Coverage Computations and Algorithms. Includes coverage computations and algorithm metrics generated by CoSMOS – percent coverage and coverage gaps, including associated statistics such as average and maximum gaps in coverage, and mean response time. Coverage computations and algorithms are defined in Section 3.1.
- 2) Minimum EIRP Computations and Algorithms. CoSMOS provides the ability to examine and optimize return communication links by allowing user to review and adjust link parameters as to minimize the user’s return link EIRP. Minimum EIRP computations and algorithms are defined in Section 3.2.
- 3) Effective Communications Time/Throughput Computations and Algorithms. Effective communications time is defined as the actual time that a user mission can transfer its payload data through the selected network. It accounts for not only for acquisition time but also for network overheads which can have a large impact on throughput and potential limitations on the slew rate of parabolic and electronically steerable antennas. Effective communications time/throughput computations signal power analysis computations and algorithms are defined in Section 3.3.
- 4) User Burden Computations. User burden computations include antenna size and weight for parabolic, patch, dipole and electronically steerable antenna systems. In addition, coverage reductions due to potential steering and slew rate challenges for parabolic antennas are also estimated in this section. User burden computations are defined in Section 3.4.
- 5) Data Analytics Computations and Algorithms. CoSMOS leverages regression models and supporting logic, to estimate the performance for unmodeled mission scenarios. Data analytics functions and algorithms are defined in Section 3.5.
- 6) System Performance Comparison Algorithms. CoSMOS provides algorithms which compare system performance based on user selected criteria. The user has the ability to identify inputs that guide a ranking of the systems. System performance comparison algorithms are defined in Section 3.6.

2 DOCUMENT TREE AND REFERENCES

2.1 Document Tree

This ADD is one of the documents supporting users of CoSMOS. As shown in Figure 2-1 **Error! Reference source not found.**, the first level of documentation for users includes the CoSMOS User’s Guide and Release Packages which describe how to use the tool and the most recent additions to CoSMOS, respectively. The ADD, the Modeling Approach Document and the Database Information Document are second level documents which describe the tools “under-the-hood” or underlying functionality. The ADD describes algorithms and equations that are used to generate results displayed in CoSMOS, including performance metrics computations, link analyses, antenna calculations, coding and modulation algorithms, power amplifier calculations and ranking methods. The Modeling Approach Document describes the

approaches used to generate the source models and data for CoSMOS. The Database Information Document defines the database structure used by CoSMOS.

Information on the systems modeled is accessible through the library function. Future documentation may also expand to include the software architecture and test procedures and results.

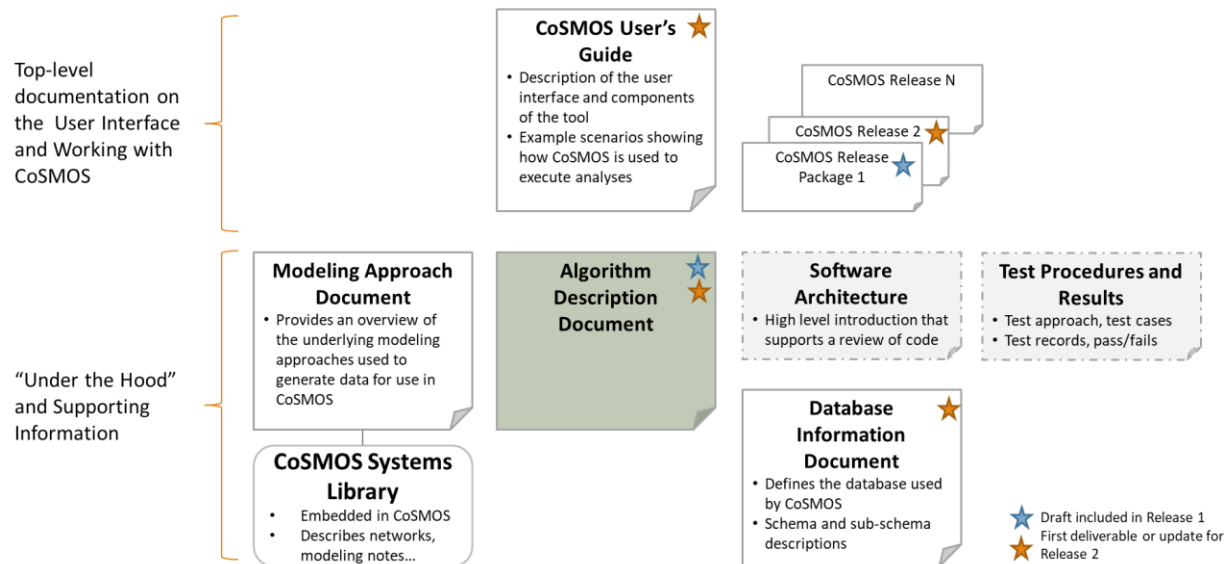


Figure 2-1: CoSMOS Documentation

2.2 References

Documents referenced in the construction of CoSMOS and/or in the description of algorithms within the ADD, including the following:

- [1] NASA, "Future Mission Space Communication and Navigation Needs, Version 2.0," NASA Space Communications and Navigation Program, 2016.
- [2] D. P. A. T. K. M. Price, "Mass and Power Modeling of Communication Satellite," NASA, Cleveland, 1991.
- [3] M. O. Courseware, MIT, [Online]. Available: https://ocw.mit.edu/courses/aeronautics-and-astronautics/16-851-satellite-engineering-fall-2003/assignments/ps4_cs_solution.pdf.
- [4] J. R. E. D. F. P. J. J. Wertz, Space Mission Engineering: The New SMAD, Hawthorne, CA: Microcosm Press, 2011.
- [5] K. & G. D. Yazdandoost, "Simple formula for calculation of the resonant frequency of a rectangular microstrip antenna.," in *IEEE 5th International Symposium on Spread Spectrum Techniques and Applications*, Sun City, South Africa, 1998.
- [6] T. R. Foundation, "The R Project for Statistical Computing," The R Foundation.
- [7] NASA, "The Space Network User's Guide," NASA Space Communications and Navigation Program.

- [8] By D. Orban and G.J.K. Moernaut, "The Basics of Patch Antennas, Updated," Orban Microwave Products, 2009.
- [9] J. R. E. D. F. P. J. J. Wertz, Space Mission Engineering: The New SMAD, Hawthorne, CA: Microcosm Press, 2011.

3 COSMOS CALCULATIONS AND ALGORITHMS

CoSMOS computations and algorithms utilize mathematical functions which process results from orbital dynamics models, dynamic link analyses models, signal acquisition models and network models. Currently, the data used by CoSMOS for its analytical processing comes from simulations using models created using Systems Tool Kit (STK), MATLAB, and NS3. Models and data generated by other tools could also be used as long as these adhere to CoSMOS input data structure.

The algorithms described in this section are generally interdependent, processing simulation results stored on its database before providing the CoSMOS user with a predicted performance assessment. A high-level depiction of this flow is shown in Figure 3-. As depicted, the majority of information presented on the CoSMOS UI is provided by the Analytics Algorithms box, which requires the input from multiple other algorithms—some of which are dependent on even other algorithms.

Section 3.5, “Data Analytics Computations and Algorithms” expands on the methodology used by the analytics algorithms to effectively predict the results of each of the supporting algorithms for user missions where no simulation data. The only output metrics that are not dependent on CoSMOS analytics algorithms are those corresponding to potential antenna specifications, as these can be determined through the calculations described in Section 3.4, “User Burden Computations” and do not require simulation data.

Finally, since CoSMOS provides the user with an option to compare various communication Section 3.6 describes an optional ranking algorithm to organize results based on user-defined importance. While the ranking algorithm does not produce any outputs, it acts as an optional means of organizing all other outputs listed in Figure 3-.

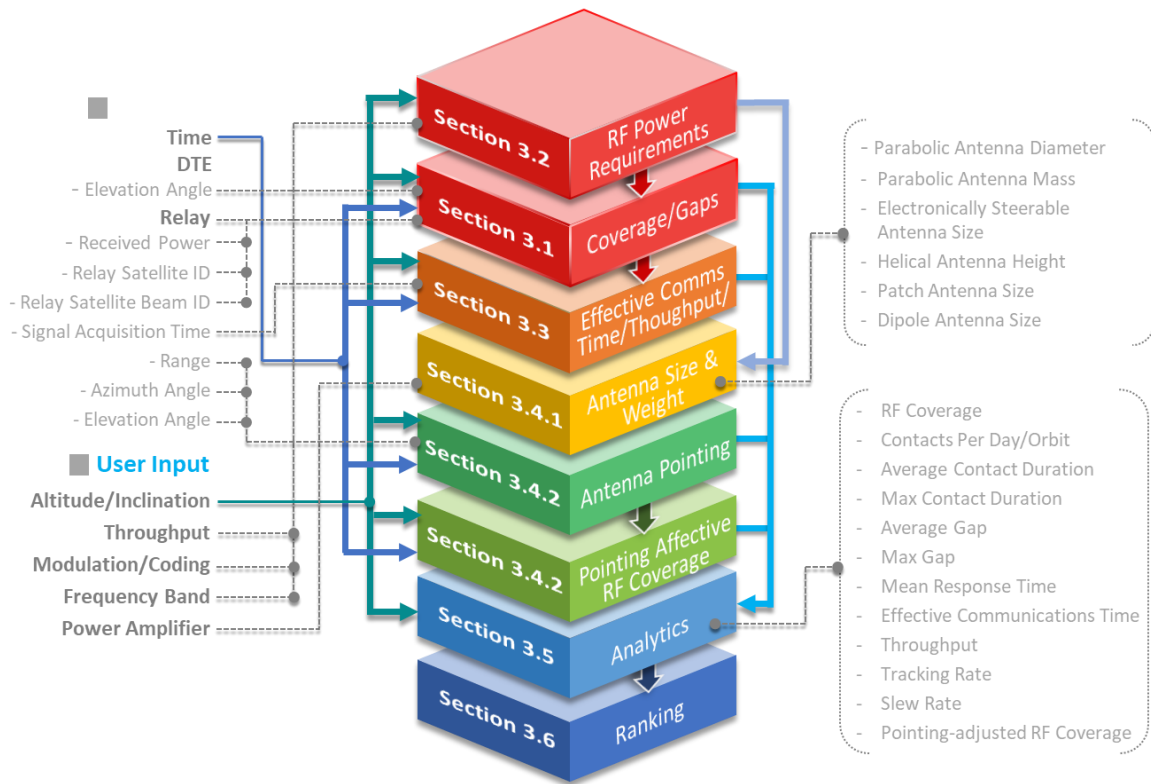


Figure 3-1: Depiction of CoSMOS Interconnectivity

3.1 Coverage Computations and Algorithms

3.1.1 Coverage

Coverage represents the duration that a user satellite has sufficient signal power to close the communications link with a given communication system over a defined period of time. This time period does not include the impacts of other factors such as network protocols overhead and mobility management functions that could reduce the coverage time in which data flow is actually feasible.

The current methodology for computing coverage for relay systems is coupled with getting simulation runs that already include the power received (P_{rec}) by the user satellite. That is, a dynamic link budget output is necessary. The modeling tool's link parameters must match CoSMOS link parameters for that specific system. This method of determining coverage was adopted because of the popular use of spot-beams by commercial satellite systems. Using purely geometric outputs from the orbit modeling tool for non-spot beams systems will be investigated in the next version of cosmos.

As such, for space-based relay systems, coverage is expressed as a percentage of the observation period, and is determined in one of two ways by comparing P_{rec} measurements reported by simulation results:

- 1) a purely geometric coverage based on the relay satellite look angle of its service link, or
- 2) a minimum power received threshold coverage computation based on the relay antenna gain patterns.

In both cases, at each time step, if the power received at the relay is equal or better than the required threshold, and the margin on the link is sufficient, the user satellite at that time step has coverage. The

resultant coverage metric (% coverage) summarizes the accumulated performance over the scenario interval. As such, space-based relay system coverage can be expressed as:

$$C = \sum \frac{t_{l(Prec > Threshold)} - t_{l-1}}{t_{max}} \quad \text{Equation 3- 1}$$

Where t_i is a timestep observation from the simulation results, and t_{max} is the final timestep value, i.e. the simulation duration.

Individual coverage events following this definition are tracked and have their durations averaged, providing the user with a sense of typical coverage duration $C_{average}$.

$$C_{average} = \frac{c}{c_{total}} \quad \text{Equation 3- 2}$$

Where c_{total} is the total number of contact events throughout the simulation duration.

The total number of individual coverage events are divided by the duration of the reference mission's orbital period to determine a typical number of relay contacts per mission orbit c_{orbit} , providing the user with a sense of contact or necessary handover frequency.

$$c_{orbit} = \frac{c_{total}}{\frac{t_{max}}{P}} \quad \text{Equation 3- 3}$$

Where P is the user satellite's orbital period defined as:

$$P = \frac{2\pi}{\sqrt{\frac{\mu}{A^3}}} \quad \text{Equation 3- 4}$$

Where μ is the gravitational constant for earth equal to $398600.4 \text{ km}^3/\text{s}^2$, and A is the user satellite orbit semi-major axis defined as:

$$A = 2(R_0 + alt) \quad \text{Equation 3- 5}$$

Where R_0 is the radius of the earth equal to 6378km, and alt is the user satellite altitude in kilometers. Note that this equation assumes a circular user satellite orbit, which is currently the only satellite mission orbit type supported by CoSMOS.

Space-based relay system coverage events are further tracked in CoSMOS by their associated relay satellite, and, when applicable, specific antenna beam for the purpose of determining the occurrence of network handover protocols as part of computing the effective communications time in **Section 3.3**. For DTE systems coverage is expressed in literal minutes per day, averaged, assuming that communications are established at any time for which the mission satellite is above the pointing elevation restrictions associated with various frequency bands—a process similar to the geometry-based coverage definition method for space-based relay systems. Individual coverage events for these systems are also tracked for the purpose of reporting their average duration.

For DTE, coverage can be expressed as:

$$C = \sum \frac{t_{l(\theta > Pointing \text{ Restriction})} - t_{l-1}}{T_{days}} \quad \text{Equation 3- 6}$$

Where T_{days} is the number of days over which the simulation occurs. We then use a daily period instead of an orbital period to obtain the number of contacts per mission orbit. .

$$c_{daily} = \frac{c_{total}}{T_{days}} \quad \text{Equation 3- 7}$$

The inputs and outputs for coverage computations and algorithms are summarized in Table 3-1. Inputs from simulation results data and from the user are listed. Outputs are listed to both the user interface and to other algorithms.

Table 3-1: Coverage Computations and Algorithms Inputs & Outputs

Inputs	
Simulation Results	CoSMOS User
Coverage data for each commercial system and reference user including the result of radiofrequency (RF) link modeling as described in the Model Description Document which will be available at CoSMOS Release 3.	None
Outputs	
CoSMOS User Interface	To Other Algorithms
None	<p>Coverage event information → to pointing rate calculations</p> <p>Schedule of coverage events & provisioning relay satellite & beam IDs → to effective communications time calculations</p> <p>Projected coverage metrics provided by each commercial system associated with the user mission orbit</p> <ul style="list-style-type: none"> • Coverage, C • Mean contacts per orbit / Day, C_{orbit} / C_{daily} • Average contact duration, $C_{average}$

The Assumptions and limitations of the coverage calculations and algorithms are as follows:

- The coverage results from the physical link model are based on a set of assumptions for the user RF transmitter capability consistent with the FCC filings or open-source documentation for each respective commercial system. As such they are representative only and are intended for comparative purposes.
- The described methodology for determining mean contacts per orbit does not account for coverage events spanning multiple orbits, i.e., if a mission orbit and relay orbit are similar enough that the user were to remain in a single relay's service zone for more than one orbital period. Due to this, an evaluation of mean contacts per orbit for a space-relay based commercial system cannot differentiate between low contact estimations due to rare coverage events and extended coverage events.
- When analyzing coverage provided by combinations of multiple DTE ground stations, time intervals during the observation period for which the user mission would be provided coverage by multiple stations is only considered once; i.e., overlaps in coverage provision are taken into account when providing performance evaluations. For the purpose of calculating ground station contacts per orbit, overlapping stations are only counted towards the summation of total contacts if the associated coverage event provides any amount of service that is *not* overlapping with another ground station.

3.1.2 Coverage Gap Metrics

From the physical link model, information is derived not only to support coverage percentage over time, but also maximum and average gap times and distributions thereof. The intent of providing gap metrics is to provide further insight into a system's ability to meet latency requirements. Latency, as defined in [1], is the allowable time to deliver data, "typically measured from the time of platform measurement to the time of delivery to its destination. The network portion is measured typically from the time of receipt of data from the platform to time of delivery to the user MOC." For the purposes of this algorithm, we consider how the distribution of gaps in RF coverage contributes to total latency as shown in Figure 3-**Error! Reference source not found.** The network portion, i.e., the flow of packets from the relay to the MOC after reception is not addressed in CoSMOS.

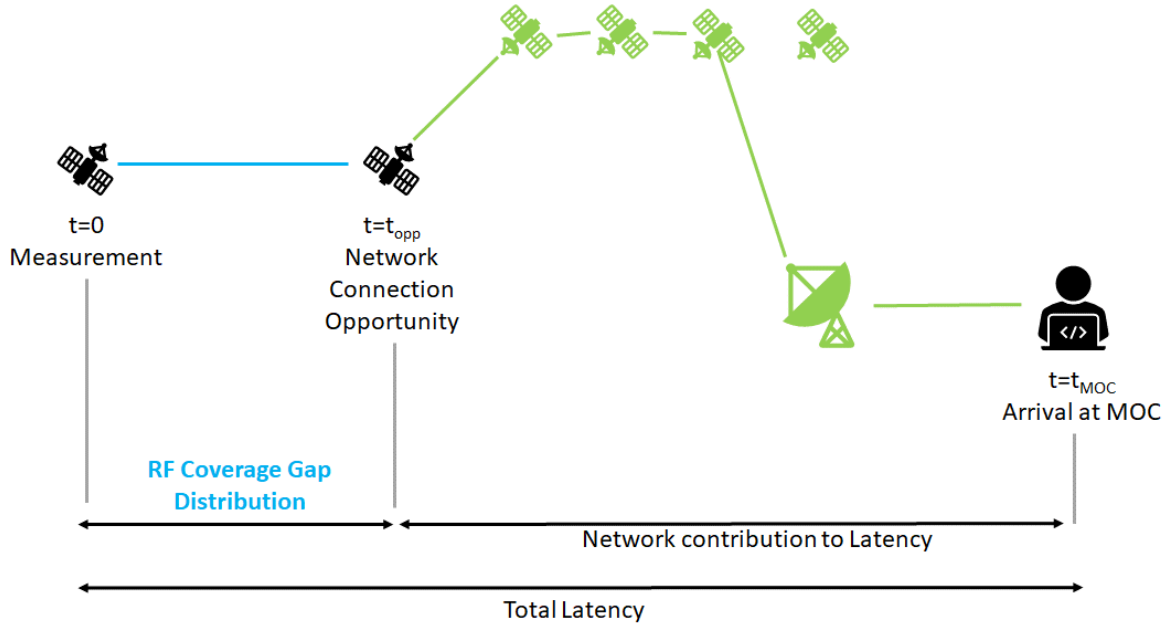


Figure 3-2: Illustration of Latency Contributions

Coverage Gap observations are summarized via several analysis methods of individual gap events across each scenario:

- Average Gap Duration, $\text{Gap}_{\text{average}}$: Determined by **Equation 3-8**, averaging the durations of individual non-coverage events as defined above as the inverse of coverage events described in 3.1.1.

$$\text{Gap}_{\text{average}} = \frac{t_{\text{max}} - C}{\text{Gap}_{\text{count}}} \quad \text{Equation 3- 8}$$

Where $\text{Gap}_{\text{count}}$ is the number of distinct non-coverage periods observed in the simulation.

- Maximum Gap Duration, Gap_{max} : The longest duration of individual non-coverage events observed.
- Mean Response Time, MRT: The typical amount of time between any point during the observation until the next coverage event. The literal equation determining this value is described in **Equation 3-9**, where Gap_i is each individual gap duration within an

experimental observation, and t_{\max} is the total duration of the simulation over which observations were made.

$$MRT = \sum \frac{Gap_i^2}{2t_{\max}} \quad \text{Equation 3- 9}$$

The inputs and outputs for coverage gap computations and algorithms are summarized in Table 3-2. Inputs from simulation results data and from the user are listed. Outputs are listed to both the user interface and to other algorithms.

Table 3-2: Coverage Gap Metrics Computations and Algorithm Inputs and Outputs

Inputs	
Simulation Results	CoSMOS User
<ul style="list-style-type: none"> Set of RF coverage gap data for each communication system (result of physical link modeling) 	<ul style="list-style-type: none"> None
Outputs	
CoSMOS User Interface	To Other Algorithms
<ul style="list-style-type: none"> None 	<ul style="list-style-type: none"> Projected RF Coverage Gap metrics provided by each communication system associated with the user mission orbit. <ul style="list-style-type: none"> Average gap duration, Gap_{average} Maximum observed gap duration, Gap_{\max} Mean response time, MRT

Assumptions/Limitations

As user mission altitude increases towards the observed commercial network's relay altitude, coverage events become less frequent and thus shorter observational periods become less representative. Thus, the closer a user mission comes to the servicing relay satellites, the longer the observations the GAM training data must be derived from, otherwise resulting in a significant margin of error that is not reflected in the summary metrics.

3.2 RF POWER

RF power requirements computations and algorithms consist of a grouping of tightly coupled functions which estimate the user satellite minimum EIRP requirement to close the communication link.

This section provides details on the minimum EIRP calculations performed by CoSMOS and its automatic coding and modulation optimization algorithm.

3.2.1 Minimum EIRP Calculation

In this section we will first calculate the minimum required EIRP for a DTE Space-to-Ground Link (SGL) and then extend these calculations to both regenerative and bend-pipe space-based relay systems. A link analysis structure is shown for context as these are used to provide the CoSMOS end user with insight into closing the communication link.

3.2.1.1 DTE Minimum EIRP Calculations

For calculating the minimum user EIRP of a DTE SGL, we first calculate the slant range distance between the user satellite and the ground terminal and then we calculate the Free Space Loss (FSL). The slant range distance is calculated from the following equation based on the user satellites orbit and frequency band elevation angle:

$$S = \sqrt{(R_0 * \cos(\Theta))^2 + a^2 - R_0^2 - R_0 * \cos(\Theta)} \text{ (km)} \quad \text{Equation 3- 10}$$

Where,

a = Distance between the Earth's geo-center and satellite (km) = altitude (km) + R₀

R₀ = Distance between the Earth's geo-center and ground station (km)

Θ = Elevation Angle (deg)

Once the slant range of the user satellite has been calculated the Free Space Path Loss (FSPL) can be calculated from the following equation:

$$\text{FSPL} = 32.45 + 20 * \log(S) + 20 * \log(\text{SGL Frequency}) \text{ (dB)} \quad \text{Equation 3- 11}$$

Where,

S = Distance between user satellite and ground terminal

SGL Frequency = Satellite to Ground Link Frequency

Once the FSL has been calculated, is the received power at the user relay terminal (P_{rec}) is determined as follows:

$$P_{\text{rec}} = 228.6 - G/T + IL + \text{Required} \frac{E_b}{N_o} \text{ (dBW)} + 10 * \log(\text{Data Rate}) \text{ (dBW)} \quad \text{Equation 3- 12}$$

The minimum EIRP can then be calculated as follows:

$$\text{EIRP}_{\text{min}} = P_{\text{rec}} + \text{FSPL} + AL + PL + ML + TPL \text{ (dBW)} + \text{Margin} \quad \text{Equation 3- 13}$$

Where:

AL = Total Propagation Losses

PL = Polarization Loss

ML = Miscellaneous Losses

TPL = Total Propagation Loss

A CoSMOS user can use the ML parameter to account for anything else that has not been explicitly identified including:

- **User Spacecraft Passive Loss**
- **User Spacecraft Pointing Loss**
- **Ground Station Passive Loss**
- **Ground Station Radome Loss**
- **Ground Station Pointing Loss**

Note that future versions of CoSMOS are planned to have a more comprehensive set of link items and the user will have the capability of entering and renaming multiple additional items.

Table 3-3 depicts a CoSMOS DTE link budget and defines associated variables and constants.

Table 3-3: DTE Link Budget

	Link Budget Item	Source / Computation
1.	EIRP (dBW)	10+3+2+5+6+12
2.	Polarization Loss (dB)	Assumption
3.	Free Space Path Loss (dB)	See Equation (2)
4.	Slant Range (S_{DTE})	See Equation (1)
5.	Multipath Loss (dB)	Assumption
6.	Propagation Losses (dB)	Based on ITU-R P.618-9
7.	Gateway G/T	Network Defined
8.	Boltzmann's Constant	-228.60
9.	C/N _o (dB)	2+9+10
10.	P _{rec} (dBW)	See Equation (3)
11.	Implementation Loss	Assumption
12.	Miscellaneous Losses (dB)	User Defined
13.	User Constraint Loss (dB)	User Defined
14.	D _r (dB-bps)	$10 * \log_{10}(\text{Data Rate} * 1000)$ (dB-bps)

15.	E_b/N_o into Demodulation (dB)	9-13
16.	Required E_b/N_o	Derived from Modulation / Coding
17.	Net E_b/N_o (dB)	16-13-11
18.	Margin (dB)	14-16

3.2.1.2 Regenerative Transponder Minimum EIRP Calculation

With the exception of a slant range replaced with simply the user to relay range, the minimum EIRP for regenerative transponders is exactly as the DTE minimum range calculation presented in Section 3.2.1.1, “DTE Minimum EIRP Calculations.”

The range between the user and relay satellite is calculated from the following equation based on the user satellites altitude, the relay constellations altitude, and relay antenna beam half cone angle:

$$X = \frac{(-2*R_0*cos(\Psi)) - \sqrt{(-2*b*cos(\Psi))^2 - (4*(-2*b*cos(\Psi))^2 - (a^2))}}{2} \text{ (km)} \quad \text{Equation 3- 14}$$

Where,

X = Distance Between the user satellite and relay constellation

a = Radius of the Earth + User Satellite Altitude (km)

b = a + (Relay Satellite Altitude – User Satellite)

Note also that Miscellaneous Losses can be used to account for anything else that has not been explicitly identified including:

- **User Spacecraft Passive Loss**
- **User Spacecraft Pointing Loss**
- **Dynamics Loss**
- **RFI Loss**
- **Ground Station Pointing Loss**

3.2.1.3 Bent-Pipe Transponder Minimum EIRP Calculation

For a bent-pipe transponder system, we will need to calculate the total C/N_o that results when we combine the two links in a relay system.

- 1) **The Space-to-Space Link (SSL) and the SGL for orbital users of the relay system, or**
- 2) **The Ground-to-Space Link (SSL) and the SGL for user terrestrial users.**

The C/N_o at the SGL can be calculated from the following equation:

$$C/N_o \text{ SGL} = 228.6 + \text{EIRP}_{\text{relay}} - \text{FSL}_{\text{relay-to-gateway}} - \text{PL} - \text{TPL} - \text{ML} + \text{G/T}_{\text{GS}} \quad \text{Equation 3- 15}$$

Where:

PL = Polarization Loss in the SGL

TPL = Total Propagation Loss in the SGL

ML = Miscellaneous Losses in the SGL; user defined

G/T_{GS}= Gain over Temperature of the ground segment antenna

The P_{rec @ relay} can then be calculated from the following equation:

$$P_{\text{rec @ relay}} = 10 * \log_{10} \left(\frac{\gamma * \delta * DR}{\alpha - \beta * \delta * DR} \right) \text{ (dBW)} \quad \text{Equation 3- 16}$$

Where,

$$\alpha = 10^{\left(\frac{\frac{G}{T} @ \text{relay}}{10} \right)} * 10^{\left(\frac{228.6}{10} \right)} * 10^{\left(\frac{\frac{C}{N_0} SGL}{10} \right)} \quad \text{Equation 3- 17}$$

$$\beta = 10^{\left(\frac{\frac{G}{T} @ \text{relay}}{10} \right)} * 10^{\left(\frac{228.6}{10} \right)} \quad \text{Equation 3- 18}$$

$$\gamma = 10^{\left(\frac{\frac{C}{N_0} SGL}{10} \right)} \quad \text{Equation 3- 19}$$

$$\delta = 10^{\left(\frac{\frac{E_b}{N_0} + IL}{10} \right)} \quad \text{Equation 3- 20}$$

Once the P_{rec} is calculated, we can then estimate the minimum EIRP of the user. Again, it is equal to:

$$EIRP_{\text{min}} = P_{\text{rec}} + FSPL + AL + PL + ML + TPL \text{ (dBW)} + \text{Margin} \quad \text{Equation 3- 21}$$

3.2.2 Modulation and Coding Optimization

When a system has multiple modulation and coding options, CoSMOS can automatically select the optimal modulation and coding combination that corresponds to the minimum required Eb/No. The combination of modulation and coding is also referred to as MODCOM below.

Modulation and coding optimization consist of first calculating the ratio between of user required data rate over the available bandwidth ratio ($\frac{\text{required data rate}}{\text{Bandwidth}}$) and then filtering out any modulation and coding combinations that exceed a given threshold. This threshold is referred to as a MODCOD value and it is calculated as follows

$$\text{MODCOD} = \log_2(\text{Modulation order}) \times \text{Coding rate} \quad \text{Equation 3- 22}$$

For example, the MODCOD corresponds to 16 QAM with rate 2/3 is 2.66.

Note for systems using FDMA schemes the calculated required data rate can be directly used in the required data rate to bandwidth ratio. For any system using a TDMA schemes, the required data rate is rounded up to the step size based on its frame structure.

It should be noted that for relay systems the available modulation and coding schemes are extracted from their FCC filings or system of specifications; e.g., TDRS. For DTE's, modulation coding schemes are based on the CCSDS standards as DTEs are easily upgradable.

The inputs and outputs for the coding and modulation optimization algorithms are summarized in Table 3-4. Inputs from simulation results data and from the user are listed. Outputs are listed to both the user interface and to other algorithms.

Table 3-4: Coding and Modulation Optimization Algorithm Inputs and Outputs

Inputs	
Simulation Results	CoSMOS User
<ul style="list-style-type: none"> System available bandwidth, available modulation & coding schemes, multiple access scheme. 	<ul style="list-style-type: none"> Mission specific data rate requirements, desired modulation & coding scheme
Outputs	
CoSMOS User Interface	To Other Algorithms
<ul style="list-style-type: none"> None 	<ul style="list-style-type: none"> Minimum Eb/No that passes data rate (throughput) requirements

3.3 Effective Communications Time/Throughput

Effective communications time is defined as the actual time a user can transmit its own data across a communication channel. It is the time that remains once signal acquisition and network protocol overhead are subtracted from coverage. Once effective communication time is calculated, we can accurately estimate the maximum throughput of a communication system when supported a selected NASA mission. This coverage adjustment is necessary as many commercial satellite communications systems use multiple-access schemes which will limit their throughput for space communications applications.

3.3.1 Effective Communications Time

As illustrated in Figure 3-, CoSMOS currently accounts for signal acquisition time, and network registration and re-registration when handovers from beam-to-beam movements fail as part of effective communications time calculations. These effects are taken from the results of NS3 simulations will be described in a Modeling Approach Document. For illustrative purposes, effective communications time as presented in CoSMOS can be described by **Equation 3-23**:

$$T_{EC} = C - T_{aq} - T_{net} \quad \text{Equation 3- 23}$$

Where T_{aq} is time required for a relay satellite to acquire the signal across each contact event, and T_{net} is the time required to register into the network, and losses associated with network efficiency/inefficiency; this value is unique to each network model.

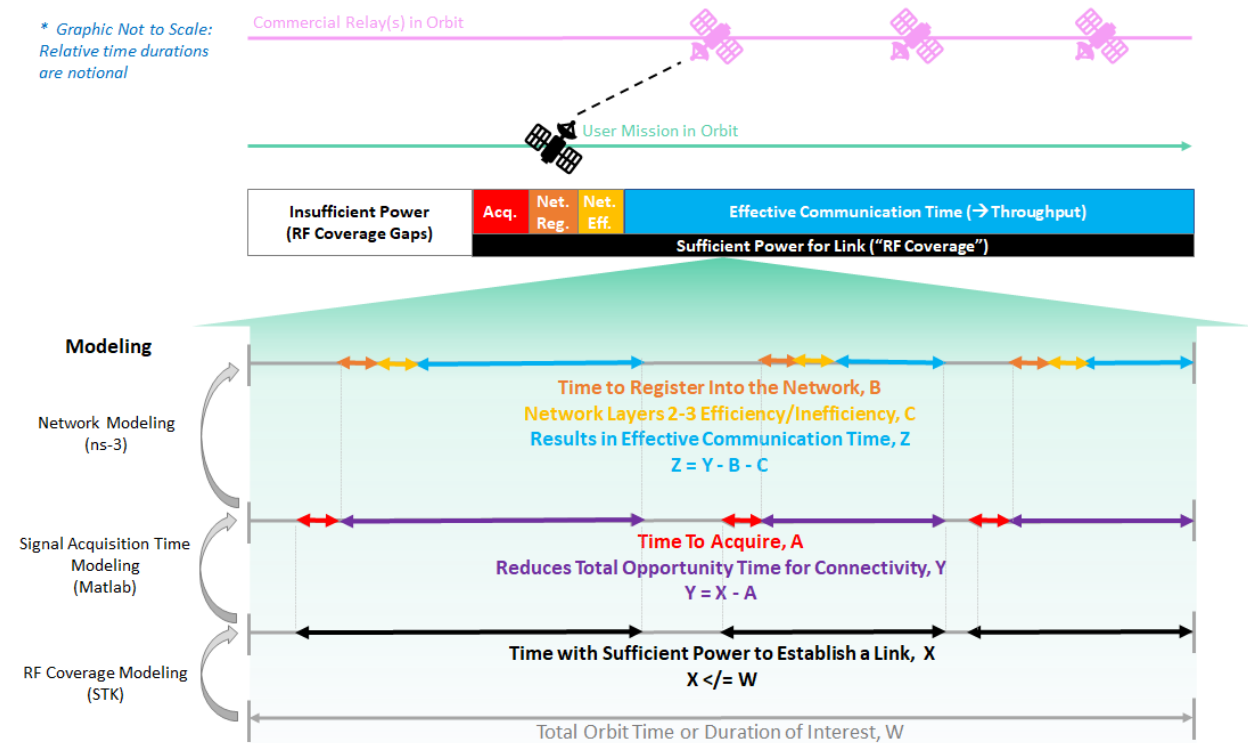


Figure 3-3: Modeling and Relationships between Technical Performance Evaluation Components

The inputs and outputs for the effective communication time computations are summarized in Table 3-5. Inputs from simulation results data and from the user are listed. Outputs are listed to both the user interface and to other algorithms.

Table 3-5: Effective Communications Time Inputs and Outputs

Inputs	
<ul style="list-style-type: none"> Simulation Results 	CoSMOS User
<ul style="list-style-type: none"> Schedule of RF Coverage events & provisioning Relay Satellite & Beam IDs (from RF Coverage definition algorithm) Acquisition time T_{aq} from MATLAB models Network registration and re-registration metrics (NS3) 	<ul style="list-style-type: none"> N/A
Outputs	
CoSMOS User Interface	To Other Algorithms
<ul style="list-style-type: none"> N/A 	<ul style="list-style-type: none"> Effective Communication Time, T_{EC} to throughput calculation, Section 3.3.2

Assumptions/Limitations

- The current effective communication time computation assumes that the communications network is not saturated, and the user can receive access upon request or when scheduled.
- DTE “network” utilization is considerably simpler than relay-based systems intended to support a multitude of simultaneous users, and for this purpose impacts of signal acquisition and communications initiation protocols have been deemed insignificant for the time being. Therefore, effective communication time is not applied to DTE systems.

3.3.2 Throughput

Throughput, or data volume in a specified time is the amount of data generated by or received by the mission user platform in a given unit of time whether status telemetry, command uploads, or mission data that needs to be transported [1]. The intent of providing this metric in CoSMOS is to present how well (or poorly) a communication system may meet a user’s expectation for data volume transmission.

Throughput is derived from the effective communication time and system data rates within the NS3 model. Specifically, CoSMOS applies the mission specific data rate determined by using the RF power requirements calculations and algorithms to the predicted effective communications time for a specific mission. This data rate is simply assumed to persist throughout the full effective communications time duration, e.g., a mission with an effective communications time equal to 40% of a given day and a maximum data rate of 100kbps will transmit at that data rate for an expected 9.6 hours each day, resulting in 3.456 Gbits of throughput per day. From this maximum throughput calculation, the user can specify a lower value for daily throughput and results will be propagated through to determine EIRP requirements. As such, throughput is expressed as:

$$\text{Throughput} = T_{EC} * DR_{max} \quad \text{Equation 3- 24}$$

For DTEs, throughput is based purely on coverage instead of effective communications time. When multiple DTE ground stations are used to support a user mission, each ground station’s individual data rate and coverage time is used to provide a daily throughput metric. In the event of overlapping coverage events between multiple DTE ground stations, the station with the highest data rate is considered ‘active’ for the duration of the overlap.

The inputs and outputs for throughput computations are summarized in Table 3-6. Inputs from simulation results data and from the user are listed. Outputs are listed to both the user interface and to other algorithms.

Table 3-6: Throughput Calculations Inputs and Outputs

Inputs	
Simulation Results	CoSMOS User
<ul style="list-style-type: none">• Effective communications time prediction, T_{EC}• Maximum mission data rate, DR	<ul style="list-style-type: none">• Desired throughput (Gb/Day)
Outputs	
CoSMOS User Interface	To Other Algorithms
<ul style="list-style-type: none">• Estimated throughput (Gb/Day)	<ul style="list-style-type: none">• None

Assumptions/Limitations

Results of individual ground station throughput for combined DTE ground station performance observations are currently limited to the assumption of maximum achievable data rate, determined for each ground station independently. For advanced link budget or throughput customization options, ground stations must be selected individually within the CoSMOS UI. Expansion of this observation capability is planned for future releases.

3.4 User Burden

User burden calculations provided by CoSMOS include: 1) the size and weight calculations for parabolic and patch antennas, and 2) the size of dipole, helix and electronically steerable antennas. CoSMOS also provides estimates of potential coverage reduction from vehicle slew rate limitations for both parabolic and Electronically Steerable Antenna (ESA) type antennas.

3.4.1 Antenna Size and Weight Calculations

The Antenna Size and Weight Calculator uses the minimum EIRP to estimate the size for and/or weight for parabolic, patch, dipole, helix, and ESA. To estimate the required antenna gain, an amplifier value can be selected by the CoSMOS user.

Figure 3- depicts the logic flow of the CoSMOS antenna size and weight calculator. The detail calculation for each antenna is provided in Sections 3.4.1.1 through 3.4.1.5.

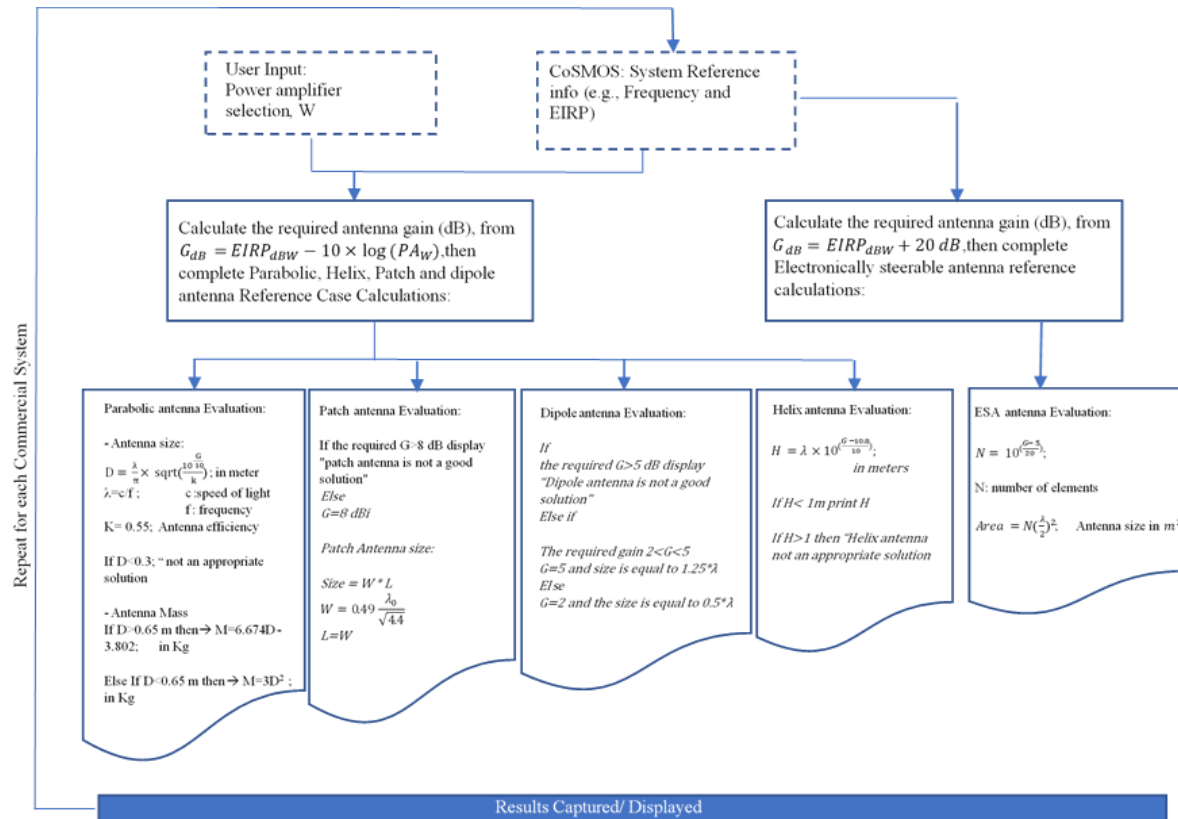


Figure 3-4: Logic Flow: Reference Antenna Size and Mass

The inputs and outputs for user burden computations and algorithms are summarized in Table 3-7. Inputs from simulation results data and from the user are listed. Outputs are listed to both the user interface and to other algorithms.

Table 3-7: User Burden Computations & Algorithms Inputs and Outputs

Inputs	
Simulation Results / CoSMOS Library	CoSMOS User
<ul style="list-style-type: none"> System frequency Calculated EIRP from minimum EIRP calculations and algorithms 	<ul style="list-style-type: none"> Antenna Power Amplifier value, PA
Outputs	
CoSMOS User Interface	To Other Algorithms
<ul style="list-style-type: none"> Size for five types of antennas <ul style="list-style-type: none"> Parabolic Patch Dipole ESA Helix Weight for two types of antennas <ul style="list-style-type: none"> Parabolic ESA 	<ul style="list-style-type: none"> Minimum Eb/No that passes data rate (throughput) requirements

3.4.1.1 Parabolic size and weight

Based on the minimum EIRP and the user given power amplifier (PA) value, the gain (G) is first calculated. The antenna size (diameter of the antenna in meters) is derived from:

$$D = \frac{\lambda}{\pi} \sqrt{\left(\frac{10^{10}}{k}\right) \frac{G}{4\pi}} \quad \text{Equation 3- 25}$$

Where λ is the wavelength of the signal in meters, D is the diameter of the parabolic reflector in meters, and k is the efficiency. By assuming an efficiency of 60% and using knowledge of the user frequency and gain, one can derive the antenna diameter (size).

For the mass of the parabolic antenna, two empirical formulas were used.

If the size of the antenna diameter is more than 0.6 meters, the mass is calculated using:

$$M = 6.674D - 3.802 \quad [2] \quad \text{Equation 3- 26}$$

where D is the antenna diameter.

If the diameter is less than 0.6 meters the antenna weight is calculated as:

$$M = 3D^2 \quad [3] \quad \text{Equation 3- 27}$$

where D is the antenna diameter and M is the antenna mass in kg.

3.4.1.2 Helix antenna size and weight

Based on the determined user required antenna gain (calculated from the minimum EIRP and the PA) the Helix antenna size is calculated as follow:

$$H = \lambda \times 10^{\left(\frac{G-10.8}{10}\right)} \quad \text{Equation 3- 28}$$

Where λ is the wavelength, and G is the required antenna gain.

It should be noted that the mass of the antenna is considered negligible for a Helix type antenna. Furthermore, if the required antenna height exceeds one meter the CoSMOS will flag the Helix antenna as not an appropriate solution.

3.4.1.3 Electronically steerable antenna size and weight

Based on the determined user required antenna gain, the electronically steerable antenna size and weight are calculated as follow:

The antenna gain is calculated as:

$$G = \text{EIRP} + 20 \quad \text{Equation 3-29}$$

Where it is assumed a 10dBm amplifier is used for any single antenna element.

$$\text{Area} = \left(N \frac{\lambda}{2}\right)^2 \quad \text{Equation 3- 30}$$

Where N is the total number of required elements and is calculated from:

$$N = 10^{\left(\frac{G-5}{20}\right)} \quad \text{Equation 3-31}$$

where N , is the total number of required elements.

A 5 dB gain for a single antenna is assumed. Moreover, the distance between elements is considered to be half of a wavelength and symmetric.

The mass of the array antenna can be calculated from:

$$M = 0.9671N - 0.1826 \quad [4] \quad \text{Equation 3- 32}$$

3.4.1.4 Patch Antenna size and Gain

A typical gain of a patch antenna is between 6-9 dB. In CoSMOS, a gain of 8dB is assumed for a typical patch antenna. As a result, regardless of the required antenna gain, the gain of the patch antenna is 8dB.

If the required gain is equal or less than 8 dB, the antenna size is calculated as follow:

$$W = 0.49 \frac{\lambda_0}{\sqrt{4.4}} \quad [5] \quad \text{Equation 3- 33}$$

By considering the length is equal to width in a rectangular patch antenna, the overall size is:

$$\text{Size} = L \times W \quad \text{Equation 3- 34}$$

In the above equation, the relative dielectric constant of the patch antenna is 4.4 which is a typical substrate's dielectric constant (e.g., FR4). A general size of a patch antenna can be calculated from an experimental equation

$$W = \frac{c}{2f \sqrt{\frac{\epsilon_r + 1}{2}}} \quad [5] \quad \text{Equation 3- 35}$$

where W is the width of the patch antenna, f is the frequency and ϵ_r is the dielectric constant of the substrate.

$$\epsilon_{eff} = \frac{\epsilon_r + 1}{2} + \frac{\epsilon_r - 1}{2} \left[\frac{1}{\sqrt{1 + 12 \left(\frac{h}{W} \right)}} \right] \quad [5] \quad \text{Equation 3- 36}$$

where ϵ_{eff} is the effective dielectric constant, and h is the height of the substrate.

$$L = \frac{c}{2f\sqrt{\epsilon_{eff}}} - 0.824h \left(\frac{(\epsilon_{eff} + 0.3) \left(\frac{W}{h} + 0.264 \right)}{(\epsilon_{eff} - 0.258) \left(\frac{W}{h} + 0.8 \right)} \right) \quad [5] \quad \text{Equation 3- 37}$$

Where L is the length of the patch antenna.

If the required gain is more than 8 dB, a patch antenna is not sized and, therefore, not recommended.

3.4.1.5 Dipole Antenna size and Gain

There are two specific sizes of dipole antennas that are frequently used because of their efficiency, antenna patterns and gain properties:

1. A dipole antenna with the size of $1.25 * \text{Lambda}$ and a gain of 5 dB,
2. A dipole antenna with the size of $0.5 * \text{Lambda}$ and a gain of 2 dB.

Based on the required antenna gain, one of the two options is selected by CoSMOS.

3.4.2 Antenna Pointing Requirements / Limitations

One of the potential challenges with space-based relay communications, particularly if relay communication satellites are non-geostationary, is the need for the user to continuously point a parabolic antenna to a relay satellite and to be able to rapidly switch from one passing relay satellite to another. Depending on the pointing rates between the bodies, the user may be burdened by additional hardware, mass, complexity, or alternative systems (such as phased arrays) that may not only have cost implications but will reduce coverage. CoSMOS projects the feasibility of body-pointing, mechanical pointing, or need for a phased array solution.

Pointing has both a “tracking” and “slewing” rate requirement. Tracking rate refers to the angular rate at which a user must adjust its antenna to maintain line-of-sight with a servicing relay satellite. Slewing rate refers to the speed the user mission must adjust its antenna to switch between two relay satellites, e.g., a user satellite losing coverage from relay satellite A and gaining coverage from relay satellite B. The separation of these metrics is intended to provide the user with a sense of angular intensity associated with either *holding* an active link (tracking) or *reorienting* in time to *establish* a new link (slewing).

STK only reports angular relationships in terms of relative azimuth & elevation angles, and as such it is limited in its ability to report angular changes across timesteps. To obtain a direct angular change between mission-to-relay, instantaneous recordings of Azimuth & Elevation relationships were made at “coverage transition events”. These events are points in time during the simulation at which RF Coverage is either transferred between different relay satellites, dropped, or initiated, following definitions of coverage provision described in Section 3.1.

The determination of both tracking and slewing rates is described by the equations below:

$$Pr = \frac{\zeta}{t_i - t_{i-1}} \quad \text{Equation 3- 38}$$

Where t_i is the simulation time at which the coverage transition event is observed, and ζ represents the non-Azimuth/Elevation constrained angular change between coverage transition events described as

$$\zeta = \arccos\left(\frac{R_{i-1}^2 + R_i^2 - d^2}{2 * R_{i-1} * R_i}\right) \quad \text{Equation 3- 39}$$

Where R_i is the range from the mission satellite to relay satellite in km at coverage transition event i , and d is determined as

$$d^2 = [R_{i-1} * \cos(\Theta_{i-1})]^2 + [R_i * \cos^2(\Theta_i)]^2 - 2[R_{i-1} * \cos(\Theta_{i-1}) * R_i * \cos(\Theta_i)] * \cos(\Phi_i - \Phi_{i-1}) \quad \text{Equation 3- 40}$$

Where Φ_i and Θ_i are the Azimuth and Elevation angles respectively between the mission satellite and relay satellite for the same coverage transition event observed with R_i .

also provides feasibility of pointing for missions based off several reference COTS antenna options. Logic flow for this feasibility determination is depicted in Figure 3-.

For body pointing and tracking, industry reference points are as follows:

- < 0.5 deg/sec: Impact to spacecraft is minimal; reaction wheels may be enough for small vehicles.
- > 0.5 deg/sec: Structural impact on appendages, weight and cost increases; gyros and/or thrusters are required.

Body pointing for communications purposes also must be balanced against compatibility with the science mission and observations. If time is taken away from scientific observation to point for communications, this can be viewed as another type of burden.

Figure 3- provides mechanical specifications for several commercially available products. The tracking rates for these COTS products vary from 0.02 deg/sec to 3.75 deg/sec, all exceed 4kg and require at least 10 Watts of power.

If neither body nor mechanical pointing is feasible, the result displays an indicator that phased array solutions could be considered. The user is provided with the predicted pointing rate (deg/s) result as reference.

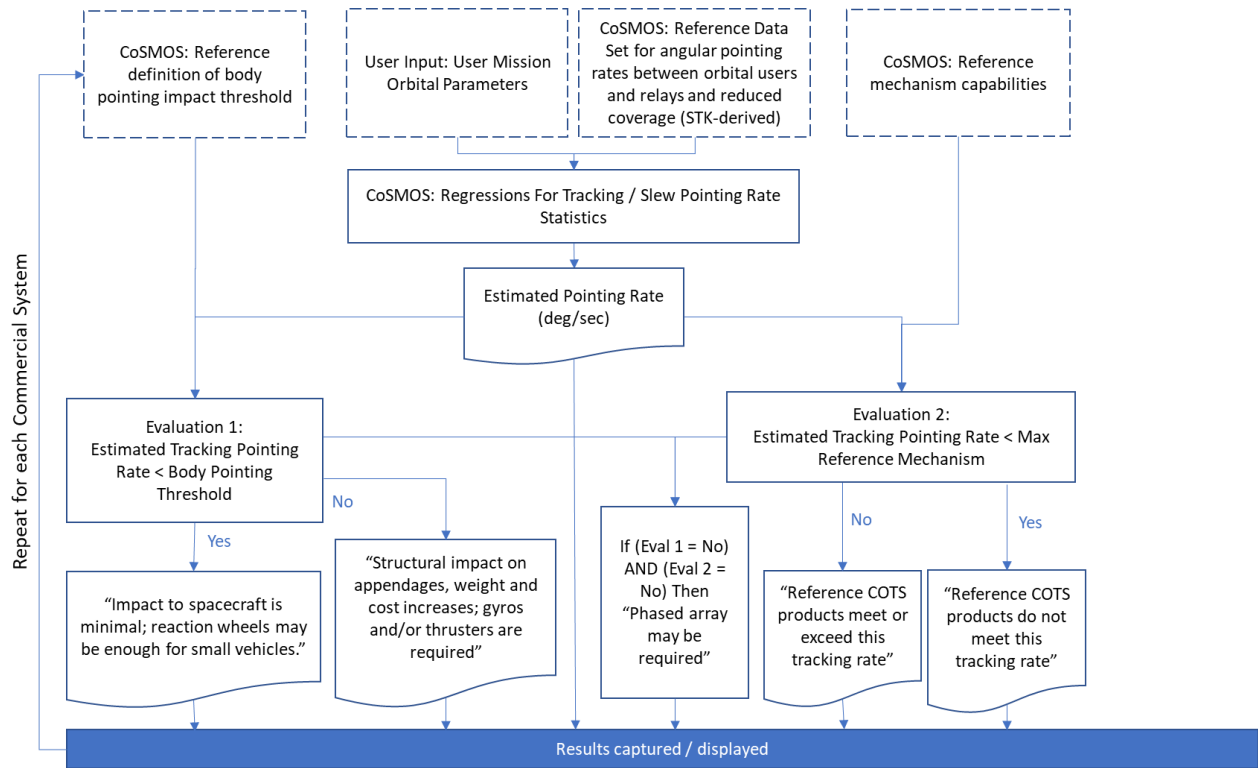


Figure 3-5: COTS pointing rate feasibility assessment algorithm

Table 3-8: Sample Antenna Pointing Mechanisms from Moog Inc.

Product #	Tracking Rate (deg/sec)	Slew Rate (deg/sec)	Mass (kg)	Power (W)	Reference Missions
Type 33-Large Range of Travel Variant	0.1	3	5.23	17	HALCA Mission – 830 kg spacecraft
Type 55	0.75	3	16.42	6.4 W/axis	ADEOS Mission – 3560 kg spacecraft
Type 33	0.02	0.075	4.6	17 W/axis	SOHO Mission – 1850 kg spacecraft
Type 22	3.75	--	5.44	10 W/axis	Earth observation satellites
Interorbit Link	0.06	0.4	15.6	14	Large GEO

3.4.3 Pointing Reduced Coverage

The average tracking rate (deg/s) plus two standard deviations provide a reference point that captures most of the distribution of rates without forcing the user burden to be driven by maximum values under the assumption of a generally Gaussian distribution. Using this reference threshold, the coverage time which falls below the reference is captured as an additional output.

Pointing reduced coverage is represented as:

$$C_{PR} = \sum C_i \wedge (Pr_{track\ i} > Pr_{threshold}) \quad \text{Equation 3- 41}$$

Where C_i is set of simulation intervals where coverage is established according to the definitions provided in **Section 3.1**, $Pr_{track\ i}$ is the set of tracking rates associated with each simulation interval as defined in **Section 3.4.2**, and $Pr_{threshold}$ is defined as:

$$Pr_{threshold} = Pr_{average} + 2Pr_{stdev} \quad \text{Equation 3- 42}$$

Pointing reduced coverage metric is intended to provide the user with a reduction in coverage associated with reasonable antenna adjustment requirements. Note that this metric does not affect any coverage or gap metric described in other sections of this document, nor effective communications time and subsequently throughput. It is only provided for reference.

The inputs and outputs for pointing reduced coverage computations and algorithms are summarized in Table 3-9. Inputs from simulation results data and from the user are listed. Outputs are listed to both the user interface and to other algorithms.

Table 3-9: Pointing Reduced Coverage Calculations & Algorithms Inputs and Outputs

Inputs	
Simulation Results	CoSMOS User
<p>CoSMOS Model Results References:</p> <ul style="list-style-type: none"> Set of angular pointing data for each commercial system and a revised estimate of RF coverage, the result of physical link modeling. <p>CoSMOS Stored Reference Data:</p> <ul style="list-style-type: none"> Descriptive statistics of user satellite pointing <ul style="list-style-type: none"> Max pointing rate (deg/s) for both tracking and slew Average pointing rate (deg/s) for both tracking and slew Standard deviation of pointing rates (deg/s) for both tracking and slew <p>Commercial product tracking rate references, of which the critical value is the maximum</p>	<ul style="list-style-type: none"> None
Outputs	
CoSMOS User Interface	To Other Algorithms
<ul style="list-style-type: none"> None 	<ul style="list-style-type: none"> Projected pointing rate (deg/sec) for both tracking and slew, PR Estimated pointing-rate-adjusted coverage based on the tracking rate average plus two standard deviations, C_{PR}

Assumptions/Limitations

- The mechanical pointing feasibility is based on industry reference points and the data set is currently relatively small; this could be expanded for more meaningful output.
- Pointing adjusted coverage limitation threshold is based on extremities observed within the provided dataset rather than any mechanical limitation that would be consistent across user missions. Expansion of this metric is planned for future releases to provide a meaningful thresholding.

3.5 Data Analytics

The current version of CoSMOS uses predictive data analytics to extend simulation results for arbitrary missions entered by the user. CoSMOS employs either interpolation or regressions to predict these missing simulation points. Both models serve as the statistical core of an analytical architecture and adapt automatically to changing input data. CoSMOS analytic capabilities can be expanded as it leverages R for all analytical functions. R is both a statistical programming language and an opensource software package (an interpreter) which CoSMOS uses as an internal analytics server.

The primary goals for the statistical models as they are to be used in CoSMOS are twofold: first, the model is to be used as a mechanism for predicting communications performance results at orbital configurations not directly simulated. Second, “tuning” should occur automatically as new data is entered so that the aforementioned predictive capability is not dependent on manual intervention.

For terrestrial user missions utilizing space based relay satellite networks, simple interpolation was used to predict performance metrics between sampled latitude / longitude locations around the globe. Results for these users are typically consistent and non-complex due to the limited geometric interactions between observed bodies (terrestrial users in these analyses are assumed immobile and at a singular ‘altitude’ of sea level). For satellite user missions, however, simulation results vary widely between systems due to the relative geometries and velocities between mobile user satellite orbits and relay satellite orbits, as well as the expanded dimensionality of observations due to user satellite altitude. For space-based relay systems, the results datasets are generally linear (exceptions for DTE systems described below) but take on significantly different shapes between representative commercial systems. For these reasons, Generalized Additive Model (GAM) regressions were used to represent performance results for user satellite missions. For DTEs, the GAM regression approach is augmented to account for a higher level of consistency in datasets with non-coverage datapoints.

The GAM is a composition of Generalized Linear Models (GLMs) associated with penalized smoothing functions. Simplistically, GAMs can be considered a regression of resulting regressions wherein several descriptor equations are constructed to describe a data set and are then each methodically weighted so that their composition describes the data set in ways that each sub-equation individually could not.

The GAM function provided by the R Mixed GAM Computational Vehicle (MGCV) package implements model fitting and prediction with enough simplification to the initial GLMs and capability for automatic determination of relevant dataset specific parameters to allow a singular form to accurately and adaptively represent many data shapes without the need for manual tuning or prior knowledge as would be the case with simply using GLMs. Detailed explanations of GAM implementation, as well as Model verification and applications can be found in Appendix B.

The simplified regression equation form used to describe performance results for satellite user missions is as follows:

$$g(E(Y)) = \xi + f_1(\text{altitude}) + f_2(\text{inclination}) + f_3(\text{altitude, inclination}) \quad \text{Equation 3- 43}$$

Where g represents the link function translating predicted values to supplied values of altitude and inclination, ξ is a conventional parametric component of the linear predictor E , and f_n represents a penalized smoothing function approximating the form of a GLM constructed relating Y to altitude and/or inclination. Specifically, f_1 and f_2 are univariate smooth functions directly relating Y to altitude and inclination respectively, assuming gaussian error distribution. When attempting to compare the effects of altitude and inclination simultaneously, it is important to consider their tensor product as opposed to a generic multivariate regression due to their disparate dimensionality (i.e. a change of 1 degree of inclination is expected to have drastically different effects on the model compared to a change of 1km in altitude). As such, f_3 associates Y with the tensor product of altitude and inclination to address this disparity.

The general form described in **Equation 3-43** is sufficient for user satellite missions utilizing relay systems. DTE system datasets, however, typically differ from those of relay systems in two important ways. First, the data gathering methodology for populating the original datasets of these systems has a significantly higher degree of consistency and certainty compared to relay system data.

Second, DTE datasets are significantly more likely than relays to contain non-coverage datapoints, i.e., some simulations will report user satellite orbital configurations with no coverage events as described in **Section 3.1** whatsoever. These datapoints are important to account for, as they often cause a highly sensitive and drastic change in system performance according to user altitude and inclination at values where user satellite orbits transition between serviceable and non-serviceable orbital configurations. This is problematic for the previously described GAM form, as this equation relies on smoothing functions to simplify the predicted data trends by assuming a simplistic linearity—an assumption that is specifically disadvantageous for describing sudden changes from consistent (non-coverage) values to less-consistent values of significantly different magnitude. To address this, datasets containing non-coverage values use an alternative GAM form capable of addressing zero-inflation to determine both the probability of these non-coverage data points existing at a specific covariate combination, as well as the expected performance value when a covariate combination is not expected to constitute a non-coverage point. These models were implemented by using the “`zipss()`”, or Zero Inflated Poisson Location Scale regression family included in R’s MGCV package. This regression style interprets input data as Poisson distributions with the intent of both predicting values, and specifically predicting “zero” values based on Zero Inflated Poisson (ZIP) modeling. The ZIP GAMs applied in CoSMOS follow **Equation 3-43** as the simplified, linear “value” predictor relating the expected output value at a particular user altitude & inclination combination, in combination with **Equation 3-44** as the probabilistic predictor relating the probability of the result value being 0 at a particular user altitude & inclination combination.

$$g(E(Y)) = \xi + f_4(\text{altitude, inclination}) \quad \text{Equation 3- 44}$$

Where f_4 is a covariate GLM function relating Y to the tensor product of altitude and inclination, similar to f_3 . Simplistically, DTE performance metrics for satellite users that have orbital configurations resulting in the inability to obtain coverage are run through two predictive processes. First, the orbital configuration is observed via **Equation 3-44** to determine if the user will achieve coverage. If the user is determined to achieve coverage of any amount, the same orbital configurations are observed via **Equation 3-43** to predict the actual value of the desired performance metric. A detailed description of the DTE prediction process, along with important notes on ZIP GAMs and implementational distinctions from Relay predictions is provided in **Appendix B**.

The inputs and outputs for the data analytics computations and algorithms are summarized in Table 3-10. Inputs from simulation results data and from the user are listed. Outputs are listed to both the user interface and to other algorithms.

Table 3-10: Analytics Computations and Algorithms Inputs and Outputs

Inputs	
Simulation Results	CoSMOS User
<ul style="list-style-type: none"> Simulation results from Model Reference Document[], interpreted by previously detailed algorithms 	<ul style="list-style-type: none"> User mission orbital parameters to sufficiently define orbit: <ul style="list-style-type: none"> Altitude (km) Inclination (deg)
Outputs	
CoSMOS User Interface	To Other Algorithms
<ul style="list-style-type: none"> Predictive results for various communications performance metrics at user supplied orbital configurations 	<ul style="list-style-type: none"> Effective Communications Time estimation to Throughput Algorithm

3.6 System Performance Comparison

CoSMOS provides ranking algorithms to allow the user to compare system results for a set of mission inputs. Currently, there is only one ranking algorithm implemented. This is the weighted metrics ranking algorithm. Other ranking algorithms will be added in the future.

The weighted ranking algorithm addresses how the results are displayed, to provide the user with an indication of “better” performance. The user is prompted to define the importance for each of the key threshold parameters: RF Coverage, Effective Comms Time, Average RF Coverage Gap, Maximum RF Coverage Gap, RF Contacts Per Orbit, RF Coverage Contact Duration, and RF Coverage Response Time. A score is created based on the weights of each parameter based on the process depicted in Figure 3-. The system with the highest score is ranked first, etc.

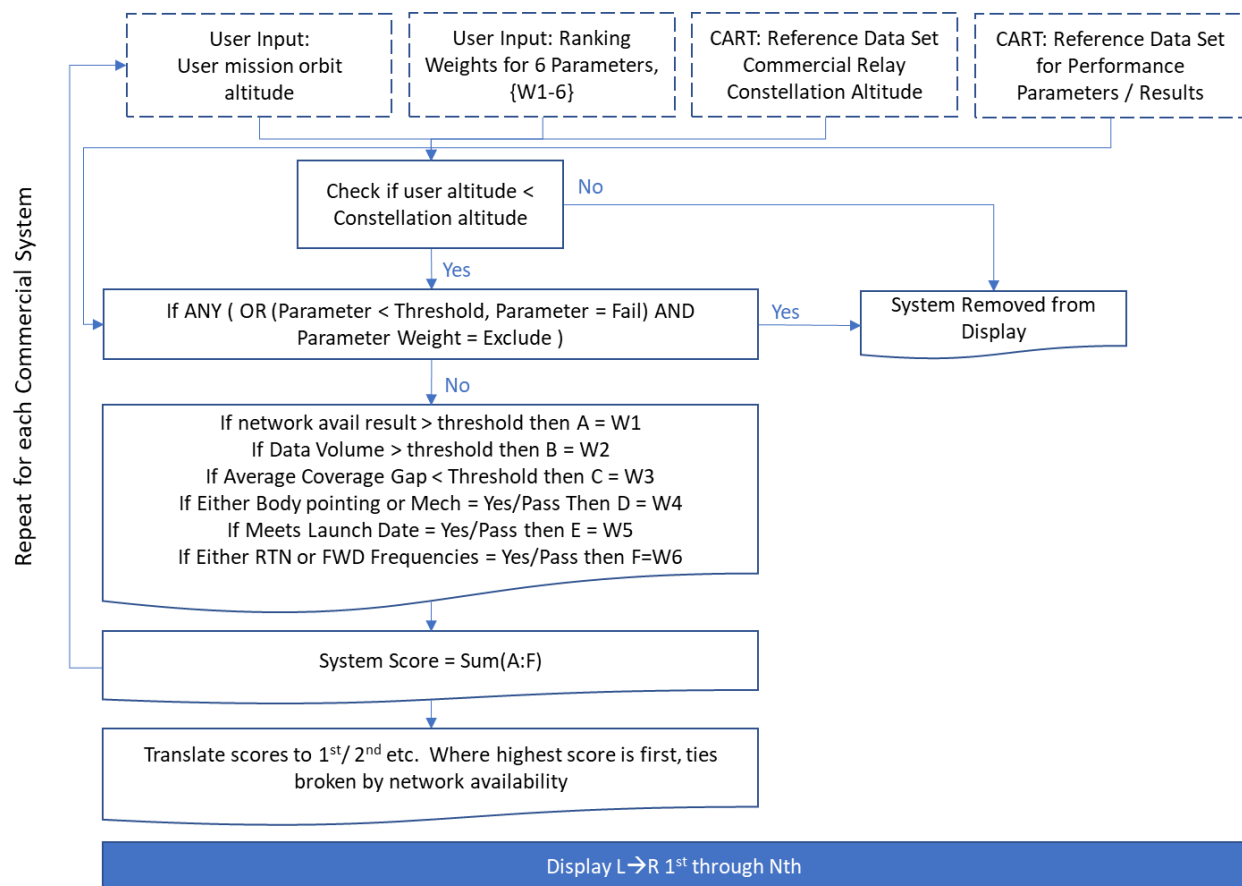


Figure 3-6: Logic Flow: Analyze / System Comparison Ranking

The inputs and outputs for the ranking algorithm is summarized in Table 3-11. Inputs from simulation results data and from the user are listed. Outputs are listed to both the user interface and to other algorithms.

Table 3-11: System Performance Algorithm Inputs and Outputs

Inputs	
Simulation Results	CoSMOS User
<ul style="list-style-type: none"> Results of analyses– e.g. performance parameters such as RF coverage, throughput, gaps, etc. 	<ul style="list-style-type: none"> Ranking preferences for seven parameters. For each parameter the user provides a qualitative weight on the relative importance as follows: <ul style="list-style-type: none"> ○ Very Important ○ Important ○ Somewhat Important ○ Not Important ○ Disregard
Outputs	
CoSMOS User Interface	To Other Algorithms

Metric results rank ordered	None
-----------------------------	------

ACRONYMS

ADD	Algorithm Description Document
CCSDS	Consultative Committee for Space Data Systems
CoSMOS	Commercial Systems for Mission Operations Suitability
COTS	Commercial Off the Shelf
DTE	Direct To Earth
EIRP	Effective Isotropic Radiated Power
EIRP	Effective Isotropic Radiated Power
ESA	Electronically Steerable Antenna
FCC	Federal Communications Commission
GAM	Generalized Additive Model
Gb	Gigabit
GB	Gigabyte
GLM	Generalized Linear Model
IL	Implementation Loss
MGCV	Mixed GAM Computational Vehicle
ML	Miscellaneous Losses
MOC	Mission Operations Center
MPL	Multi-Path Loss
MRT	Mean Response Time
NASA	National Aeronautics Space Administration
NS3	Network Simulator 3
PA	Power Amplifier
PL	Polarization Loss
P_{rec}	Received Power
QQ	Quartile-Quartile
R	Statistical Computation Software named “R”
RF	Radio Frequency
SCaN	Space Communications and Navigation
SGL	Satellite-to-Ground Link

SSL	Satellite-to-Satellite Link
STK	Systems Tool Kit
TPL	Total Propagation Losses
UI	User Interface
ZIP	Zero Inflated Poisson
ziplss	Zero Inflated Poisson Location Scale (successor to “zipls” function, seconds added for legacy reference)

GENERALIZED ADDITIVE MODEL REGRESSIONS

For terrestrial user missions utilizing space-based relay satellite networks, CoSMOS uses simple interpolation to predict performance metrics between sampled latitude / longitude locations around the globe. For all satellite user missions, CoSMOS uses Generalized Additive Models (GAMs) specifically the Generalized Additive Model (GAM).

GAMs is a composition of GLMs associated with penalized smoothing functions. GLMs in this application consist of a generalization of familiar least-squares regression used in machine learning and experimental analysis applications, that interpolate the various modeling results used by CoSMOS to arbitrary orbital altitudes and inclinations. All GLMs compute a linear predictor, a linear combination of input variables with coefficients that are ‘learned’ from data via this least-squares methodology, which is then passed through a (generally non-linear) inverse link function to obtain the mean of a certain probability distribution [5]. Once these GLMs have been constructed they are converted to a set of simplified “smooth” functions which are then fitted to relevant datasets as a singular combined descriptor function.

Simplistically, GAMs can be considered a regression of resulting regressions wherein several descriptor equations are constructed to describe a data set and are then each methodically weighted so that their composition describes the data set in ways that each sub-equation individually could not.

The GAM function provided by the R Mixed GAM Computational Vehicle (MGCV) package implements model fitting and prediction with enough simplification to the initial GLMs and capability for automatic determination of relevant dataset specific parameters to allow a singular form to accurately and adaptively represent many data shapes without the need for manual tuning or prior knowledge as would be the case with simply using GLMs.

Model Descriptions

B.1.1 Model Description: Relay Systems

Because GAMs are defined as a composition of one or more penalized GLMs, their general form is highly flexible depending on the number and nature of sub-models desired for inclusion. A simple GAM construction form, as previously described in Section 3.5, was used to avoid over-tailoring to any particular data shape while still permitting the expression of trends that do not occur across the entirety of the feature space. This simplified form is expressed below as:

$$g(E(Y)) = \xi + f_1(\text{altitude}) + f_2(\text{inclination}) + f_3(\text{altitude, inclination}) \quad \text{Equation B-1}$$

Where g represents the link function (in this case the identity link function was used making $g(E(Y)) = E(Y)$) translating predicted values to supplied values of altitude and inclination, ξ is a conventional parametric component of the linear predictor E , and f_n represents a penalized smoothing function approximating the form of a GLM constructed relating Y to altitude and/or inclination. Specifically, f_1 and f_2 are univariate smooth functions directly relating Y to altitude and inclination respectively, assuming gaussian distribution. The number of coefficients describing this smoothing function is set to the maximum supportable number of $k-1$, where k is the number of unique values for altitude and inclination respectively contained within the observed dataset. A value of 1 is subtracted from k to support the conventional parametric component α which describes the combined effects of the traditional linear intercept for all f_n . Note that while all models are assigned $k-1$ coefficients for training, depending on the datashape many of these coefficients may be penalized close enough to zero that they have no effect on the model’s effective degrees of freedom, and hence their effect on the model can be considered negligible. It is for this reason that excessively large $k-1$ values, and thus excessively large numbers of model coefficients, are not expected to result in overfitting.

f_3 associates Y with the *tensor product interaction*, specifically exclusive of the primary effects of altitude and inclination on Y independently as represented in f_1 and f_2 . The coefficient selection for f_3 borrows

from the $k-1$ values of both f_1 and f_2 for each marginal basis, resulting in a number of coefficients equal to $(k_{alt}-1) \times (k_{inc}-1)$.

For this simple form, thin plate smoothing basis was specified for each sub-function f_n for its inherent penalization to overfitting and applicability to three-dimensional representation. An additional computation permission was passed to the GAM function allowing the training process to set f_n weighting to zero when adding the individual smooth functions together. This weighting effectively removes the smooth function from the model when training fails to determine a meaningful impact, allowing simpler data shapes to be represented by reduced modeling terms and further avoid overfitting.

B.1.2 Model Description: DTE Systems

Two new GAM forms were developed for DTE systems to account for potential non-coverage datapoints. Before either form is applied to a DTE system, the dataset is first checked for data points corresponding to non-coverage simulation results.

For datasets that do not contain these non-coverage scenarios, **Equation B-1** was used for the modeling with two key differences implemented within the R script; first, the k -values are set to static values of 7 and 12 for altitude and inclination respectively across all datasets that this form is applied to. Values of 7 and 12 are also used for the tensor product portions of the form. These k -values can be left static for DTE system modeling because the data gathering methodology for these systems resulted in uniform sampling across all datasets. Second, an additional term “ $fx = TRUE$ ” was added to the f_n definitions in R. This setting instructs the parent GAM function to *not* apply smoothing parameters to each f_n during the training process. The result of this setting is a greater impact from each individual datapoint on its immediately surrounding region in the regression’s feature space; implying a “tighter” fit to the trained data points and greater risk of overfitting. These effects, while detrimental to the modeling of relay systems, are specifically desired in the modeling of DTE systems due to the aforementioned reliability of the data gathering process. Additionally, DTE datasets have an observed predisposition to more complex data shapes than those of relays, while maintaining said consistency.

For datasets containing non-coverage scenarios, Zero-Inflated Poisson, or ZIP, GAMs are used as described in Section 3.5. The ZIP GAMs applied in CoSMOS follow **Equation B-2** as the linear “value” predictor relating the expected output value at a particular user altitude & inclination combination, in combination with **Equation B-3** as the probabilistic predictor relating the probability of the output value being 0 at a particular user altitude & inclination combination.

$$g(E(Y)) = \xi + f_1(\text{altitude}) + f_2(\text{inclination}) + f_3(\text{altitude, inclination}) \quad \text{Equation B-2}$$

$$g(E(Y)) = \xi + f_4(\text{altitude, inclination}) \quad \text{Equation B-3}$$

As with the previously described GAM forms, the identity link equation was used. f_1 and f_2 are univariate GLMs relating Y to altitude and inclination respectively. Similar to the DTE modeling process described for datasets that do not contain non-coverage scenarios, each f_n is unsmoothed.

An implementation problem with ZIP GAMs is that some system performance metrics report excessively high values in non-coverage scenarios, rather than zeroes that ZIP models are specifically designed for. These high value metrics, such as Average Gap Duration, Maximum Gap Duration, and others, are the result of some time-specific observation persisting throughout the maximum duration of the observation period. To be able to predict these non-coverage scenarios without developing a completely new methodology, datasets expected to contain these ultra-high values are “inverted” before the regression is trained on them. This inversion is a simple subtraction wherein the maximum observed values become zero, and all other values are subtracted from the simulation duration. This allows the ZIP GAM to accurately predict non-coverage scenarios, although at a slight cost to accuracy in prediction of genuine coverage values.

B.1.3 Model Verification

Due to the generalized form, wide range of intended applications, and self-updating nature of the described regression modeling process, it is any attempt to verify each individual model within this document would quickly become obsolete; potentially without notice as CoSMOS is intended to accept user-supplied data without requiring back-end intervention. Instead, tools to aid the end user in assessing the quality of the GAM's application to each specific scenario are planned to be provided directly within CoSMOS and are automatically produced along with each regression model update in future releases. Information on how to interpret these tools will be provided in the CoSMOS User's Guide. This section will instead justify the usage of the described process through a sampling of outputs when applied to a diversity of data shapes to demonstrate flexibility.

Assessment of regression modeling is often subjective and difficult to quantize—especially for such a generalized methodology intended for such a wide range of unknown applications. While particularly “good” or “bad” models can be easily identified by a familiar observer viewing their results in the context of their inputs, problems arise when attempting to communicate these assessments or when attempting to identify the strengths and weaknesses of “middling” quality models. As such, objective assessments are better made with regards to specific features of the resulting model such as error spread and bias tied to their occurrence within various regions of the feature space. To aid this process, standard residual plotting techniques typically used for regression assessment are applied to each model to provide a means of evaluation at a glance.

For our assessment, the four types of residual plots use and their purpose are:

- Response vs. Fitted Values: The model's predicted coverage values (Response) against the simulation provided coverage value that the model was trained on (Fitted Values)
- Residuals vs. Linear Predictor: Relates the model's accuracy to its predicted values by plotting the model residuals (residuals) against the predicted value with which they are associated (Linear Predictor)
- Histogram of Residuals: The model residuals in histogram form
- Residual QQ Plot: Plots the residuals from lowest to highest (Deviance Residuals) against a would-be normalized scale of gaussian quantiles (Theoretical Quantiles). In a scenario where the residuals followed an ideal standard gaussian distribution, the plotted Deviance Residuals would align with the Theoretical Quantiles and follow the trend shown by the red line representing a 1:1 slope between the x and y axes

B.1.4 IridiumNext Coverage Results

Simulation reported data for IridiumNext RF Coverage demonstrate a generally consistent, linearly decreasing trend with mild curvature and low deviance across altitude or inclination trends. **Figure 0-1** shows the resulting Coverage found via simulation methodology described in **Section 3.1** represented by circular points, with the resulting GAM prediction curve for the corresponding inclinations as lines of similar color.

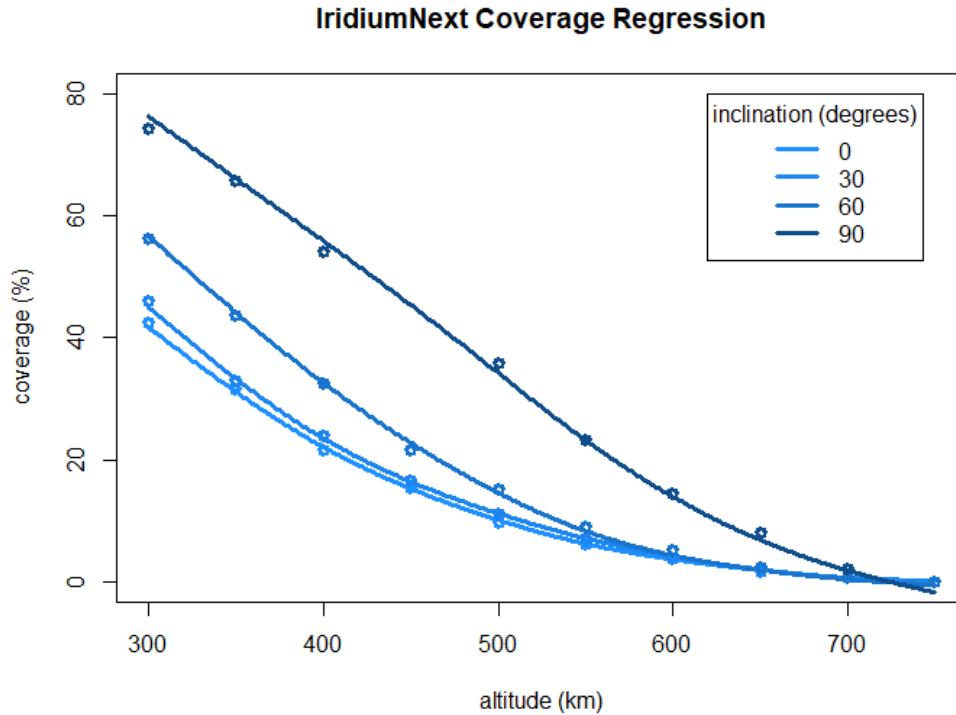


Figure 0-1. GAM regression of IridiumNext Coverage dataset with raw data points.

In this application **Figure 0-2a** shows an extremely tight responsiveness as can be seen by the near perfect linearity between the Fitted Values and Response values with minimal deviance.

Figure 0-2b in this application shows a generally tight deviance from the training values at low model predictions (residual values typically $<1\%$ below predictor values of 20% coverage) that gives way to a greater range of errors as predictor values increase, implying that the model is prone to reporting larger literal errors (up to $\pm 4\%$ coverage at high coverage estimations). Also note that the distribution of residual points is more or less evenly distributed around the 0 axis, implying minimal modeling error bias, even as the range of these errors increases at higher predictor values.

In this application the residuals can be seen to primarily fall within the $\pm 1\%$ coverage range, and all residuals fall within the $\pm 4\%$ coverage range. It can also be noted that despite the absence of any positive or negative error bias, the error distribution does not appear to be standard gaussian.

There is obvious deviance from the standard representation depicted by the red line in **Figure 0-2d**, further confirming that the distribution depicted in Figure 0-2c does not follow the standard gaussian distribution.

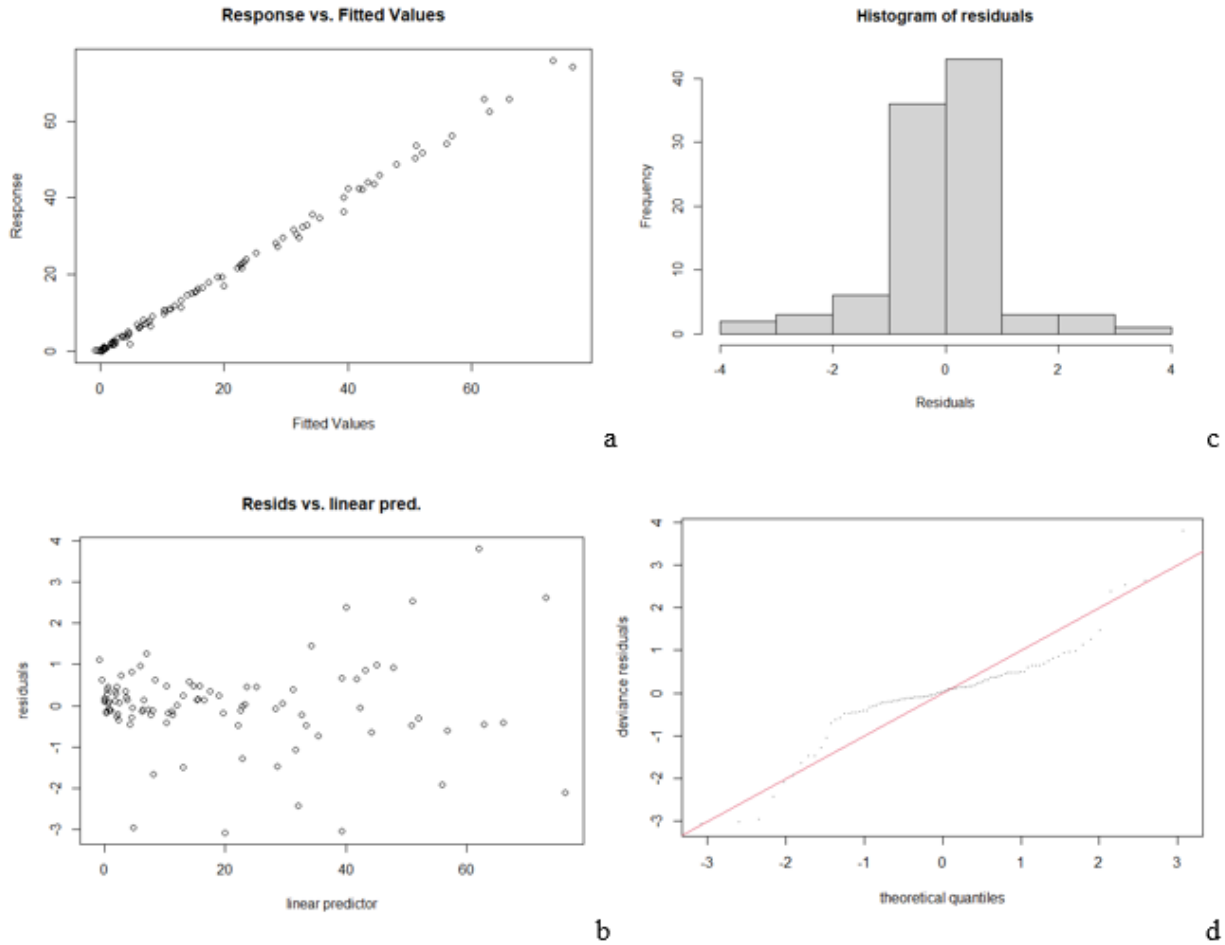


Figure 0-2. Evaluation plots for the IridiumNext Coverage regression.

In **Figure 0-2** (a) depicts the regression prediction values against the simulation provided values, (b) depicts the errors of the regression predicted values from the simulation provided values against the simulation prediction values themselves, (c) provides a histogram view of the errors between the regression values and simulation values, and (d) is the QQ Plot depicting the theoretical distribution of increasingly ordered error values against a theoretical ‘perfect’ gaussian distribution

In summary this application results in:

- Precise estimation of values that weakens as those values increase
- Tighter than standard gaussian distribution with no obvious bias

B.1.5 IridiumNext MEAN Contacts per Orbit Results

Similar to the previous dataset, IridiumNext Mean Contacts per Orbit results follow a consistent downward trend according to altitude with an inverse dependence on inclination. This inclination effect however increases quickly enough to negate the effects of altitude at high values of inclination, as can be seen in Figure B-3.

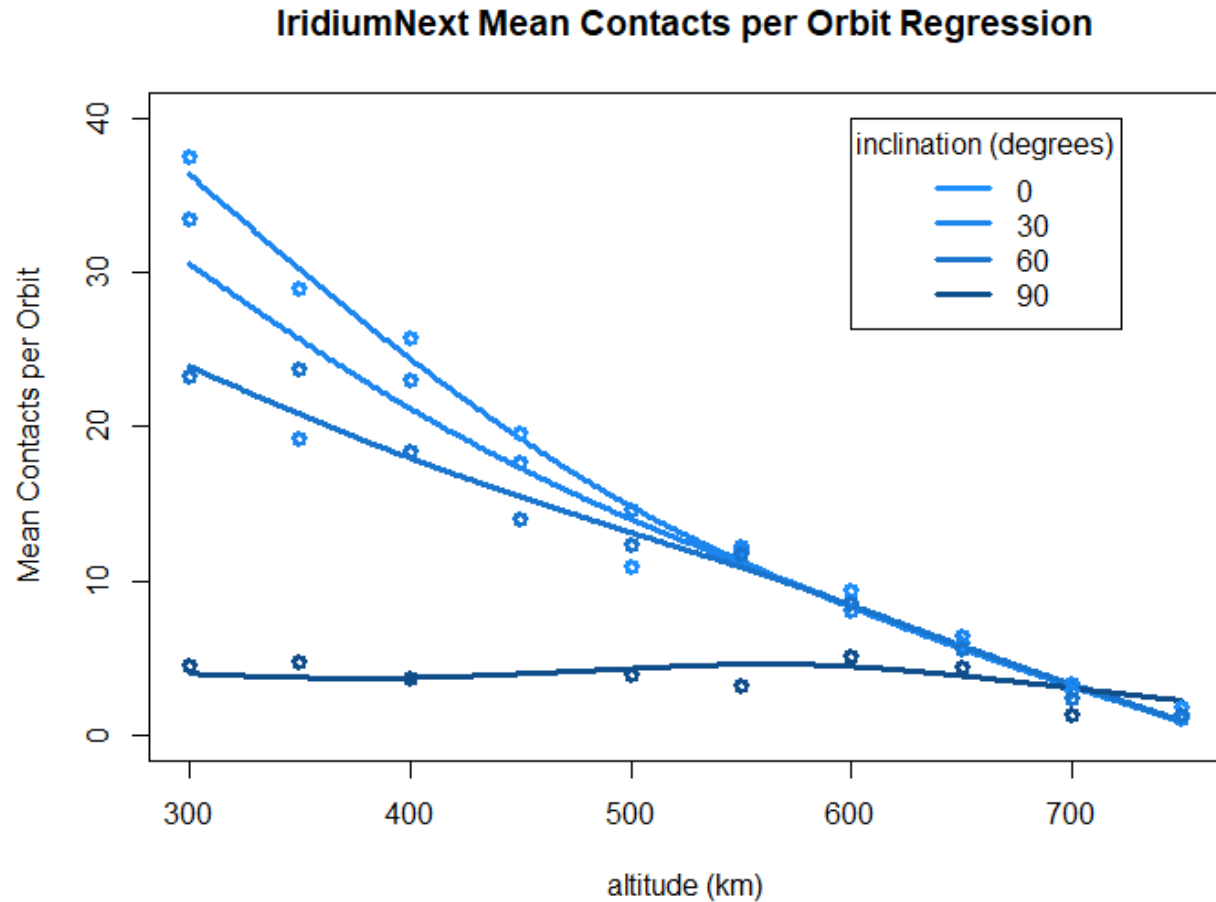


Figure 0-3. GAM regression of IridiumNext Mean Contacts per Orbit Dataset with Raw Data Points.

Figure 0-3a, b, and c show similar evaluations to their counterparts in **Figure 0-2** with a more pronounced increase in residual deviance in **Error! Reference source not found.b** suggesting a greater inaccuracy as prediction values increase, at least pertaining to literal values. **Error! Reference source not found.c** again suggests a tighter than standard gaussian distribution in residuals, as confirmed by **Figure B.4d** although not to the severity seen in IridiumNext's coverage results in **Figure B.2d**. Also notable throughout **Error! Reference source not found.a** through **Error! Reference source not found.c** is the outlier residuals of ~ -8 when the GAM predicts a value of ~ 26 , suggesting less reliable outputs at that particular region of the feature space.

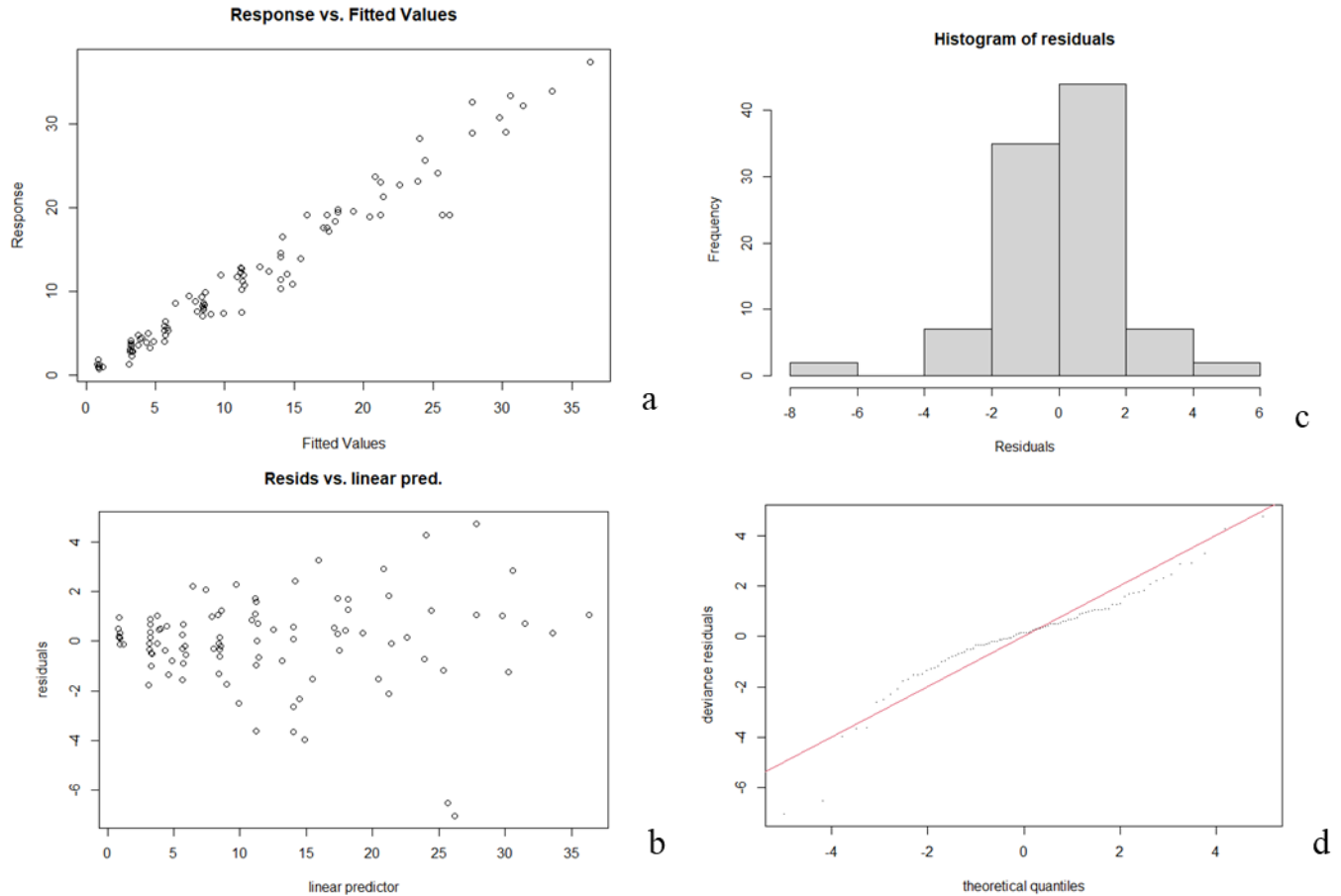


Figure 0-4. Evaluation plots for the IridiumNext Coverage regression.

In **Figure 0-4** a) depicts the regression prediction values against the simulation provided values, (b) depicts the errors of the regression predicted values from the simulation provided values against the simulation prediction values themselves, (c) provides a histogram view of the errors between the regression values and simulation values, and (d) is the QQ Plot depicting the theoretical distribution of increasingly ordered error values against a theoretical ‘perfect’ gaussian distribution

In summary this application results in:

- Somewhat precise estimation of values that weakens as those values increase
- Slightly tighter than standard gaussian distribution with no obvious bias
- Small potential for uncharacteristically large errors when the model predicts values around 25

OneWeb Mean Contacts per Orbit Results

Mean Contacts per Orbit results for OneWebMEO take a drastically different shape than the same metric for IridiumNext due to the two constellations’ similarly drastic differences in orbits. **Figure 0-5** shows a heavy quadratic-like dependence on both altitude and inclination: a distinct exponential shape can be observed across altitudes at middling inclination values, and the prominence of this effect can also be seen to vary across inclinations. The resulting regression lines are notably farther from their training data points compared to previous examples, suggesting either a worse responsivity or perhaps a less accurate fit in general.

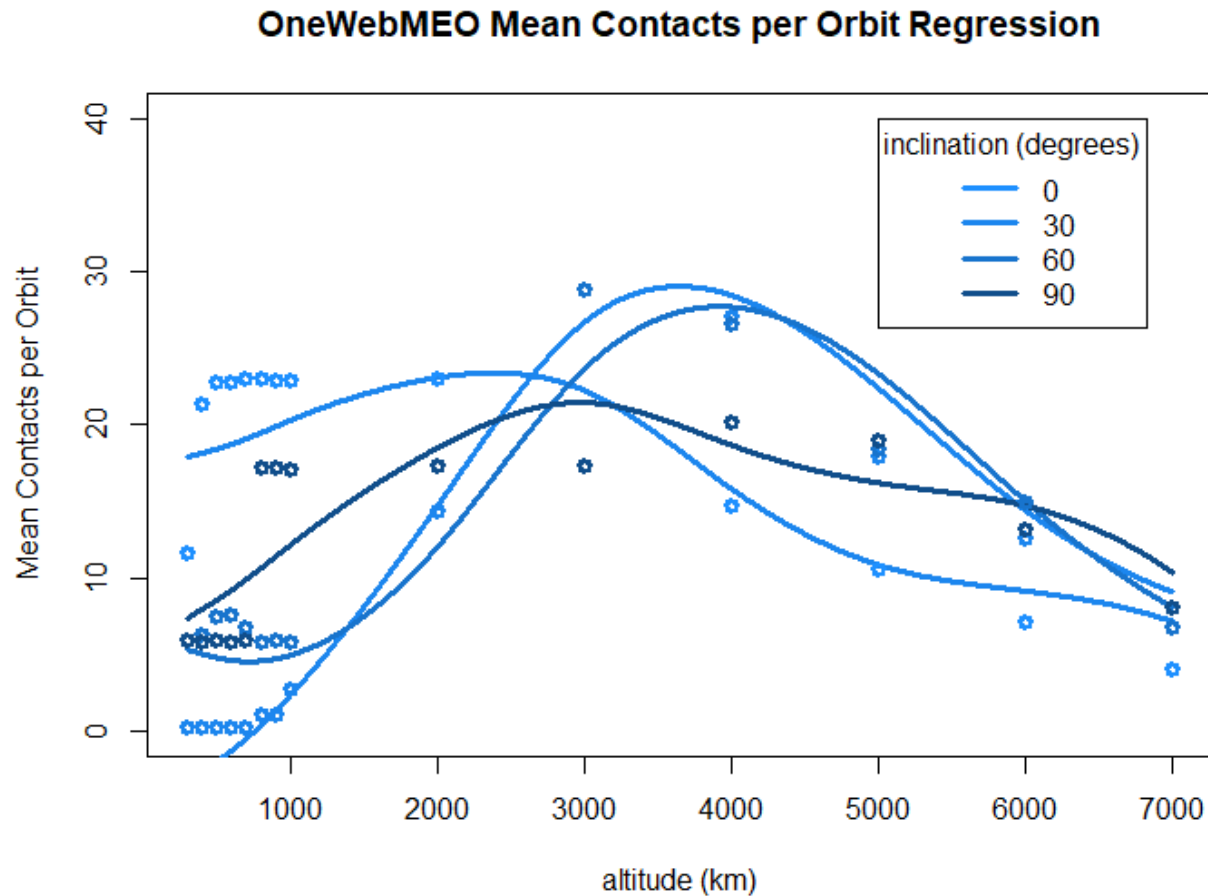


Figure 0-5. GAM regression of OneWebMEO Mean Contacts per Orbit dataset with raw data points.

Figure B.6a shows that responsivity is generally good throughout the model, although even from this view it is easy to see that experimental zero values have an excessive error range, once again showing the model's unreliability for determining non-coverage scenarios. Another notable error cluster occurs at response values of ~6. These clusters can be observed in the residuals in Figure B.6b as well, here forming diagonally decreasing lines as the linear predictor increases. The presence of these clusters suggests some aspect of the data is being systemically misrepresented by the statistical model. Referencing Figure B.5 again, it can be deduced that these clusters are likely the clusters of high-resolution sampling at altitudes between 300km and 1000km. This implies that the trend in the 300-1000km altitude range is being misrepresented by the model to various degrees depending on inclination, although no specific point is more represented than any samples beyond that range.

The fact that other residuals appear to be randomly distributed around 0 in Figure B.6b however suggests that the model presents a generally unbiased representation of the feature space as a whole. This is confirmed in Figure B.6c and B.6d which present a standard gaussian distribution of residuals across the feature space. While this distribution quality does not answer to the model's literal accuracy, it does provide assurances that the model is unlikely to be overfitted and allows a more simplistic representation of error expectations.

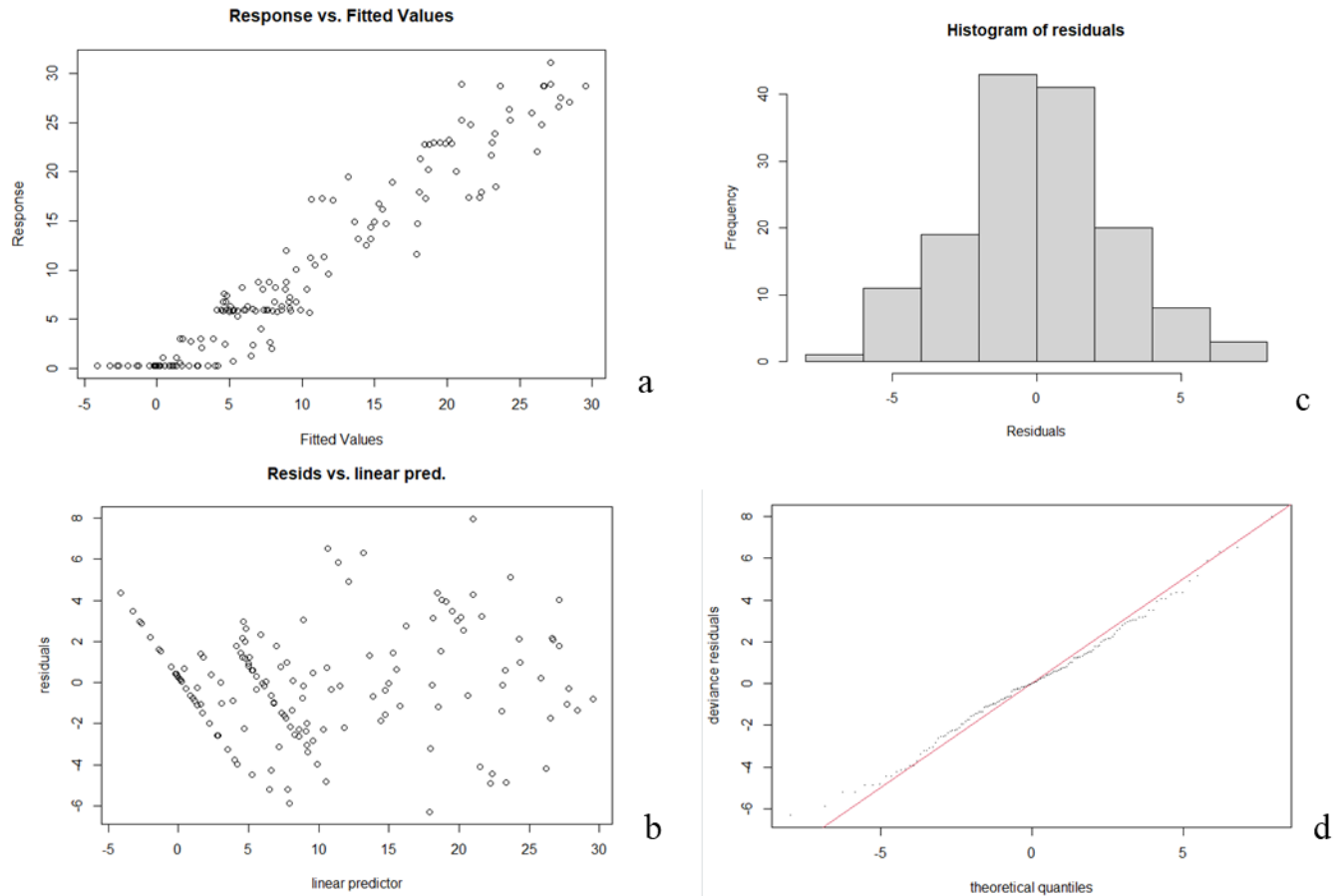


Figure 0-6. Evaluation plots for the IridiumNext Coverage regression.

In **Figure 0-6**(a) depicts the regression prediction values against the simulation provided values, (b) depicts the errors of the regression predicted values from the simulation provided values against the simulation prediction values themselves, (c) provides a histogram view of the errors between the regression values and simulation values, and (d) is the QQ Plot depicting the theoretical distribution of increasingly ordered error values against a theoretical ‘perfect’ gaussian distribution

In summary this application results in:

- A generally reliable, although not particularly precise estimation of values
 - Model predictions are specifically unrepresentative of specific trends occurring within 300-1000km altitude range
- Standard Gaussian distribution of prediction error values
- These predictions are specifically unreliable around predictions values of 0, but maintain their non-bias

DTE: Panama Coverage Results

Due to its low latitude, coverage analyses for ground stations based in Panama offer a simplistic application of the DTE GAM representation capabilities—without requiring zero value modeling since some amount of coverage is achieved at any user satellite inclination. **Figure 0-7** shows the performance of the non-ZIP model applied to the simulation results for Panama Coverage data. Note that the individual datapoints align in a much more consistent and ‘smooth’ pattern than previous relay system examples, and that the

regression lines adhere much more closely to these individual points. This tightness is a result of excluding smoothing parameters from the regression training process, which additionally results in the ‘wobbliness’ of the surface between datapoints. In typical practice this minor oscillation would be addressed by reducing the complexity, or in this case k-values, of the representative equation to be trained, but because this is a generalized form intended for application against a great diversity of datasets, such manual tuning requires a greater degree of manual intervention than can reasonably assigned to the maintenance of CoSMOS.

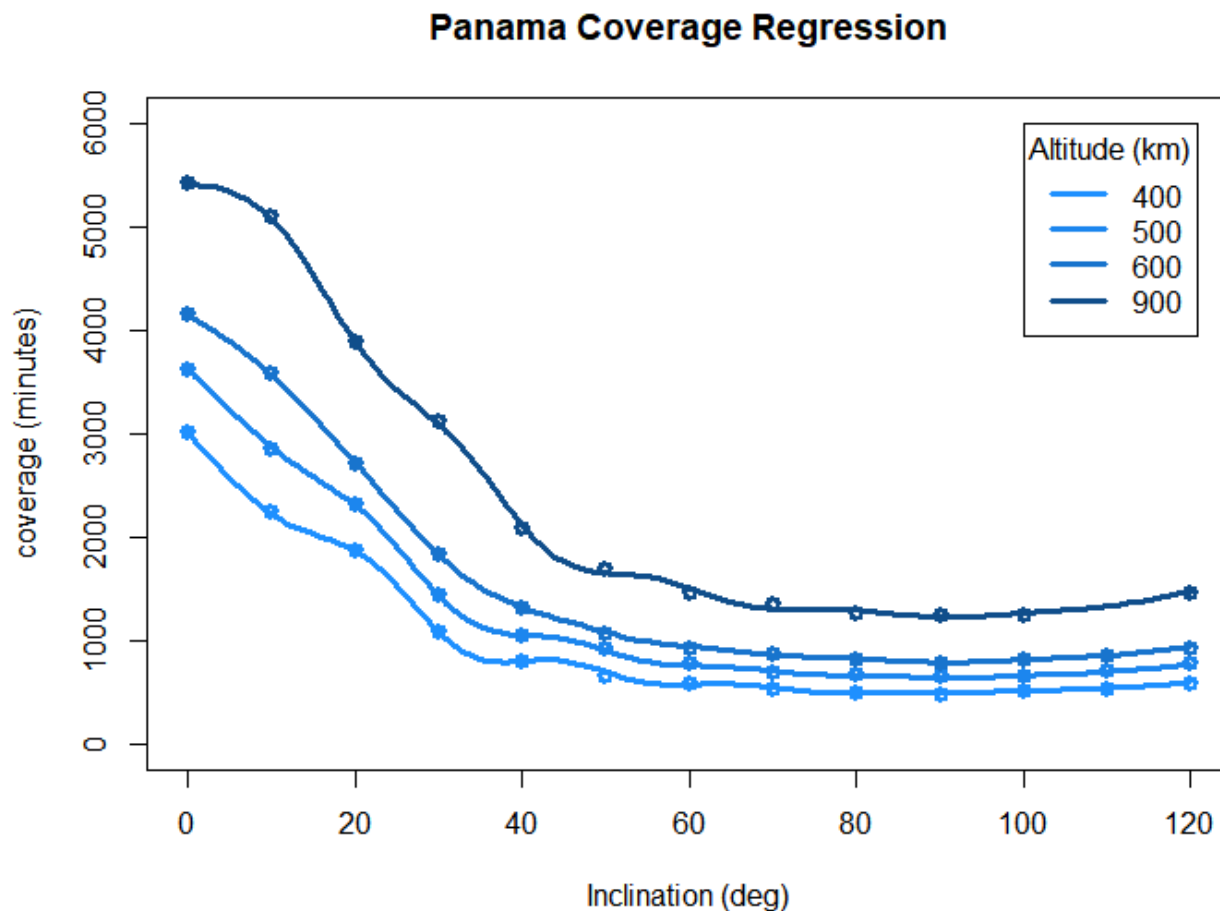


Figure 0-7. GAM regression for visibility-based coverage for a generic Panama-based ground station location over 30 days

Due to the differences in construction between DTE GAMs and relay system GAMs, performance evaluation plots previously described are unavailable. **Figure 0-8** below shows a simple boxplot distribution of literal errors in minutes between regression predicted values above and the simulated ‘real’ performance values originally used to train the regression.

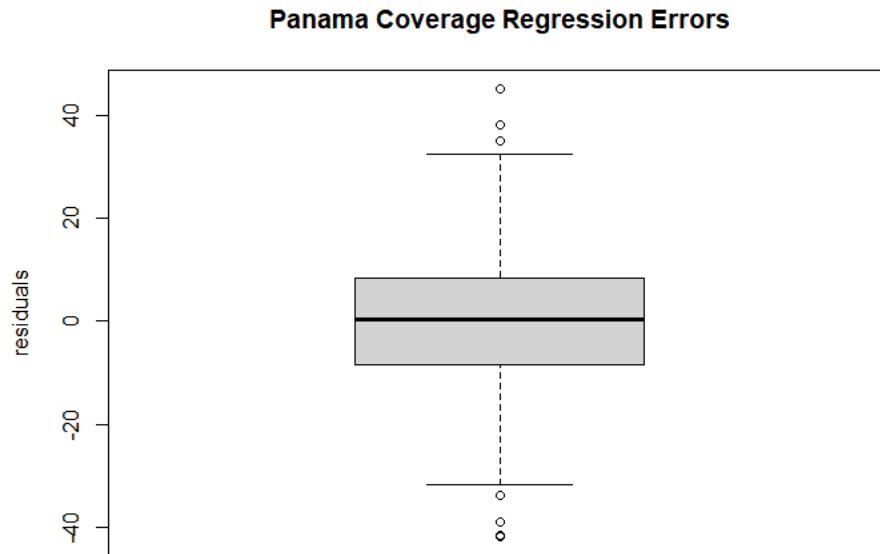


Figure 0-8. Distribution of errors between regression prediction values and simulation provided dataset.

DTE: Svalbard Coverage Results

Svalbard based station coverage results offer a simplistic view of DTE GAMs utilizing ZIP modeling to better identify points of non-coverage. Svalbard is located at a very high latitude ($\sim 78^\circ$ North) and as such is expected to be incapable of providing coverage for equatorial orbit satellite users of low enough altitude. **Figure 0-9** below confirms this as all simulation reported datapoints below 50° user inclination report 0 minutes of coverage across the entirety of the observation period. Note the regression prediction's spike in values for 900km altitude users at the edge of the non-coverage space near 60° ; this phenomenon is due to the exclusion of smoothing parameters in the non-coverage predictor portion of the ZIP model, resulting in instability at these 'crossover' regions specifically. Including the smoothing parameter for the non-coverage predictor portion exclusively has been shown to prevent these spikes, but requires a significantly greater amount of computational complexity not currently achievable by the CoSMOS server in its current state. Also note that the general 'wobbliness' of the regression has increased for this plot as well; a result of the reduced k-values and non-zero coverage values used to represent the non-zero coverage feature space.

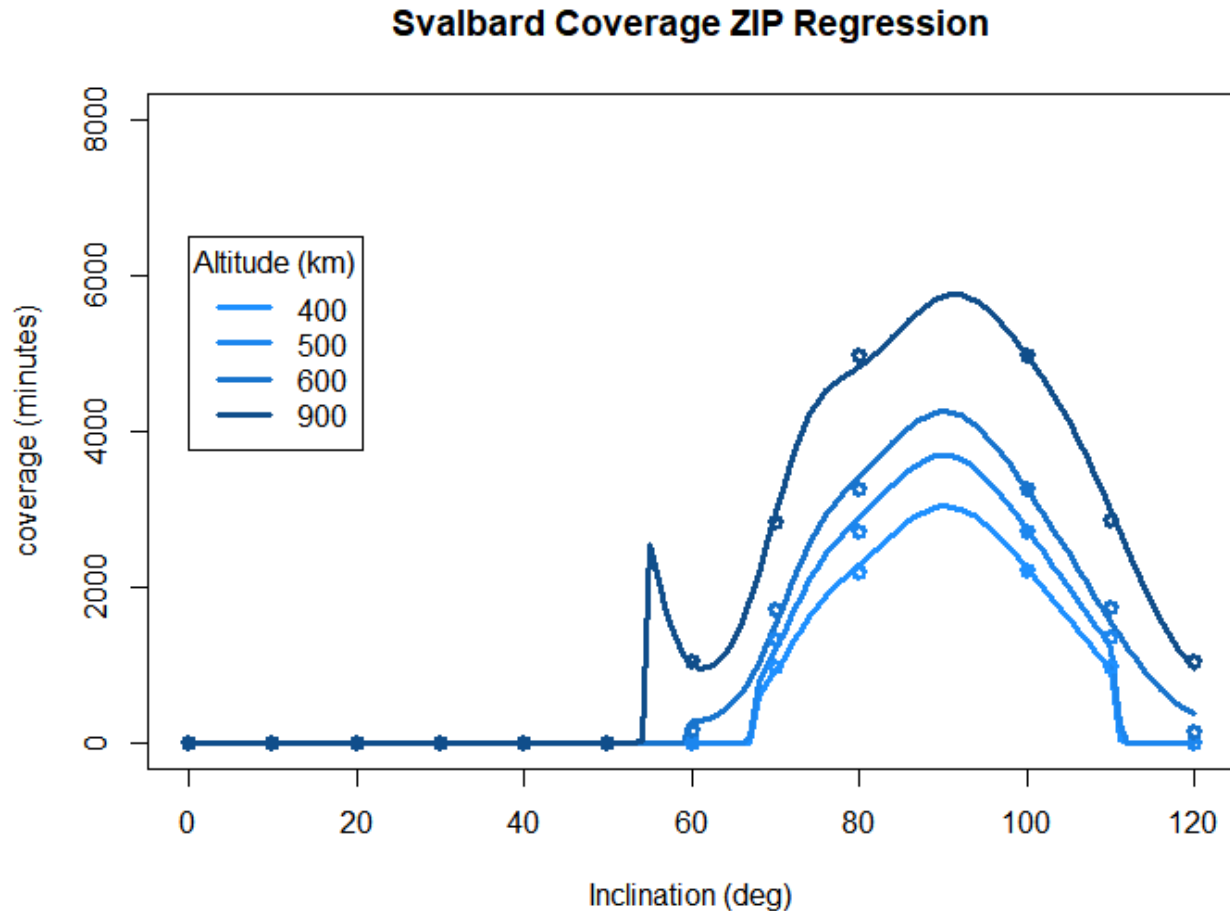


Figure 0-9. GAM regression for visibility-based coverage for a generic Svalbard-based ground station location over 30 days.

Figure 0-10 and **Figure 0-11** below show the literal regression prediction errors from the simulated data points in minutes divided into “coverage” and “non-coverage” errors respectively. Specifically, **Figure 0-10** shows the regression errors at datapoints when simulation data is greater than 0, showcasing the model’s ability to predict specific coverage values. Note that despite a similar range in prediction values to Panama data, Svalbard shows a significantly greater range in error values due to the issues mentioned above. **Figure 0-11** shows the regression errors at datapoints when the simulation data was equal to 0, meaning no coverage was reported. This plot has no spread whatsoever, meaning that all 0 values reported by the simulation data were represented by 0 values in the regression model, showcasing the ZIP model’s superior capability to represent non-coverage values when compared to the non-ZIP GAMs.

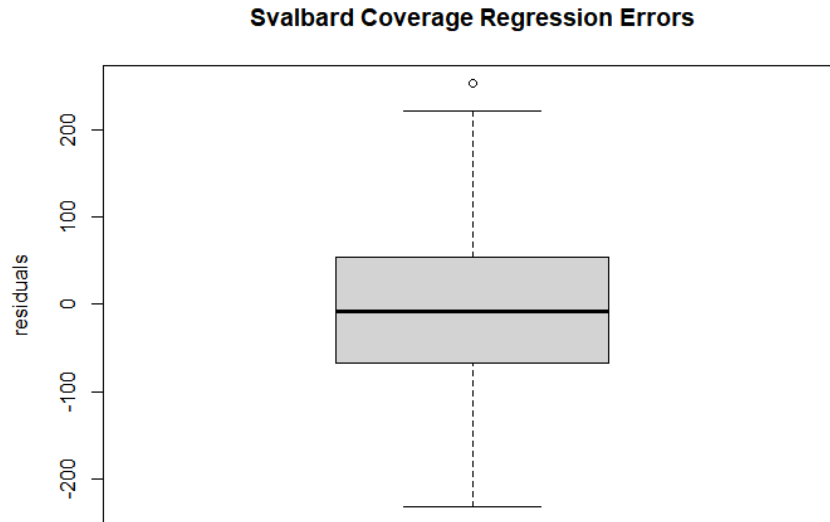


Figure 0-10. Distribution of errors between regression prediction values and simulation provided dataset at dataset values greater than 0.

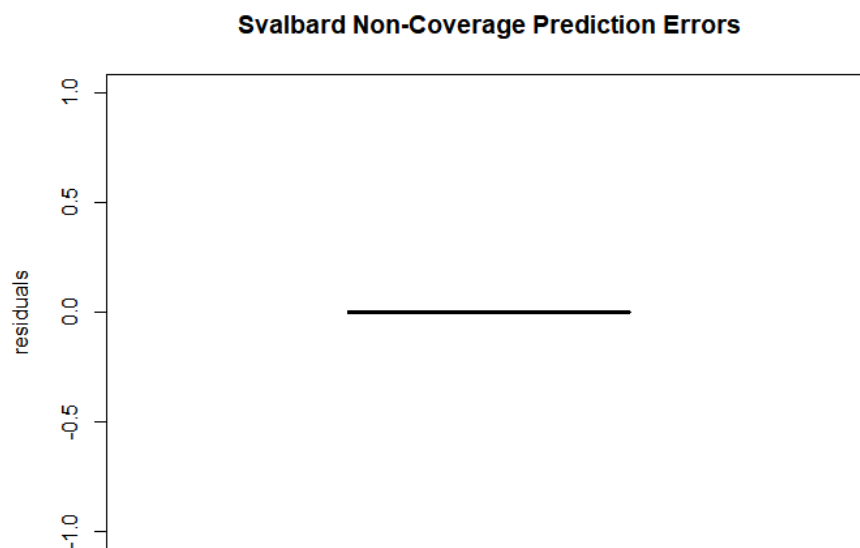


Figure 0-11. Distribution of errors between regression prediction values and simulation provided dataset at dataset values equal to 0.

DTE Combination: Svalbard + Santiago Coverage Results

To demonstrate applicability to arbitrary ground station combinations as supported by CoSMOS, Svalbard and Santiago based ground station performance data was combined by the methodology described in the Modeling Approach Document. These locations were chosen for their similarly high latitudes allowing for non-coverage scenarios in equatorial user orbits, requiring the usage of ZIP modeling. **Figure 0-12** shows the resulting regression for this combined dataset. Note that the ‘wobbliness’ has been significantly reduced due to the expanded population of non-zero coverage values within the feature space.

Combination: Svalbard + Santiago Coverage ZIP Regression

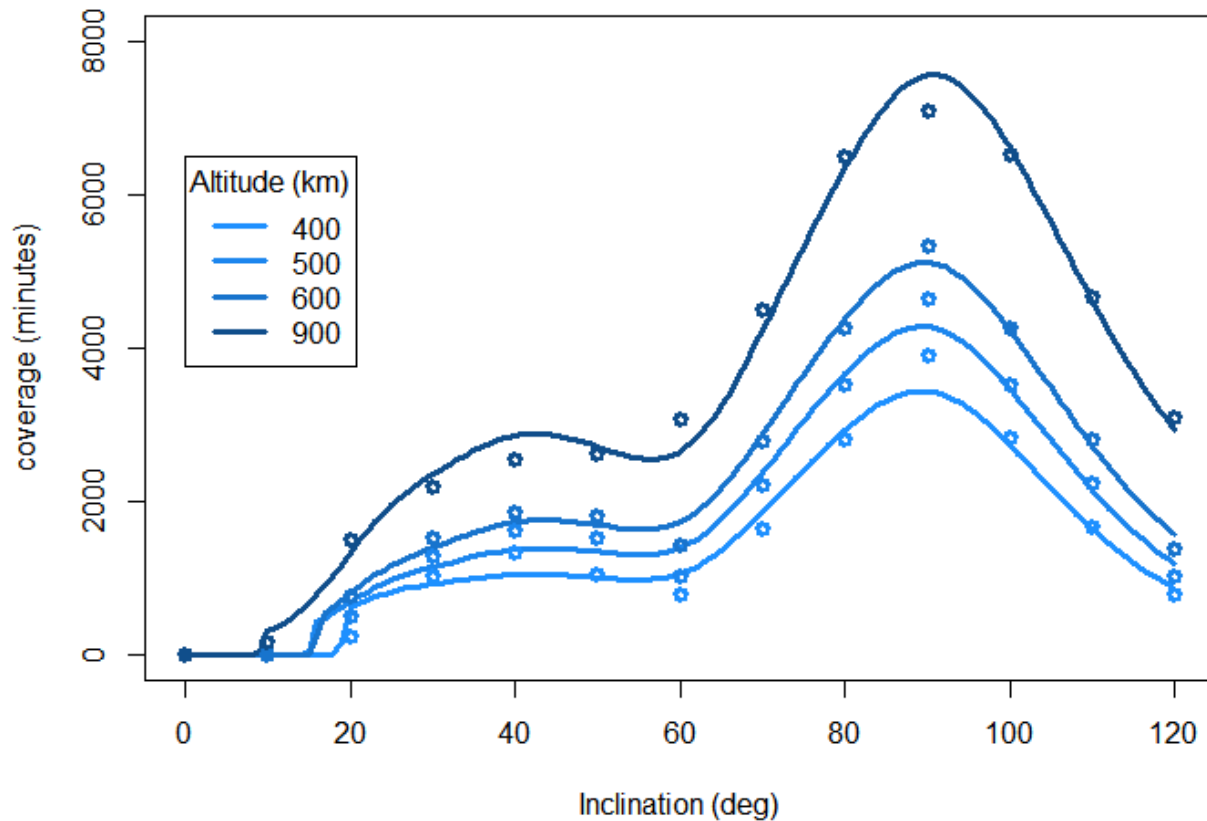


Figure 0-12. GAM regression for visibility based coverage for a summation of generic Svalbard-based and Santiago-based ground station location coverages over 30 days.

Figure 0-13 below shows a similarly large range in error values compared to that observed for Svalbard alone, suggesting that the inclusion of additional non-zero coverage values may not result in a higher dependability so long as ZIP modeling is required. **Figure 0-14** now shows a spread in error values when estimating non-coverage as opposed to the consistent 0s predicted in the Svalbard model. However, this spread is limited to values far below any meaningful error and is the result of an unstable non-coverage prediction function likely due to the low population of zero values. This instability results in the regression training process failing to determine literal zero values, and instead relying on the interaction between the linear predictor and probability predictor to generate arbitrarily very low values. For the purpose of prediction and evaluation, these values are far enough below any degree of significance ($<7e-8$ seconds per 30-day observation periods) that they can easily be considered effectively 0. This demonstrates the applicability of ZIP modeling to datasets with low enough zero-value population that their “inflation” could be considered arguable—so long as a minor degree of abstraction is applied at interpretation.

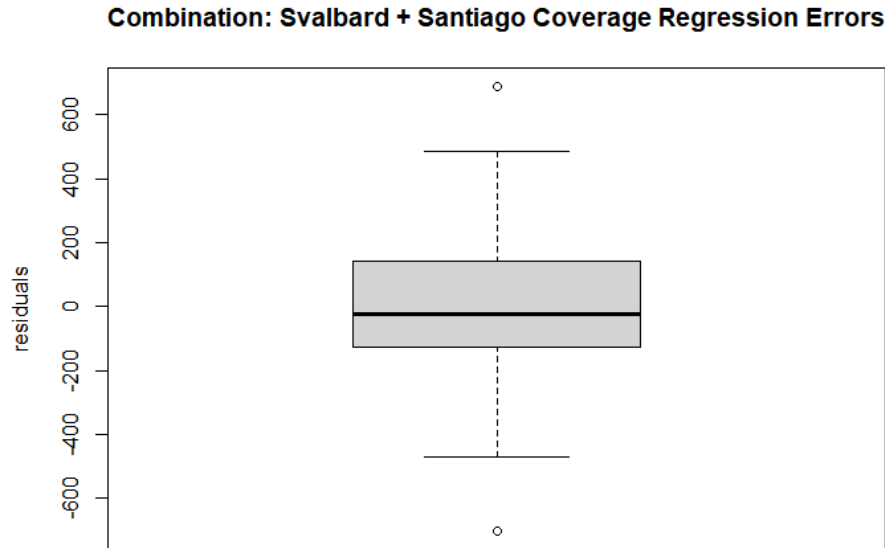


Figure 0-13. Distribution of errors between regression prediction values and simulation provided dataset at dataset values greater than 0.

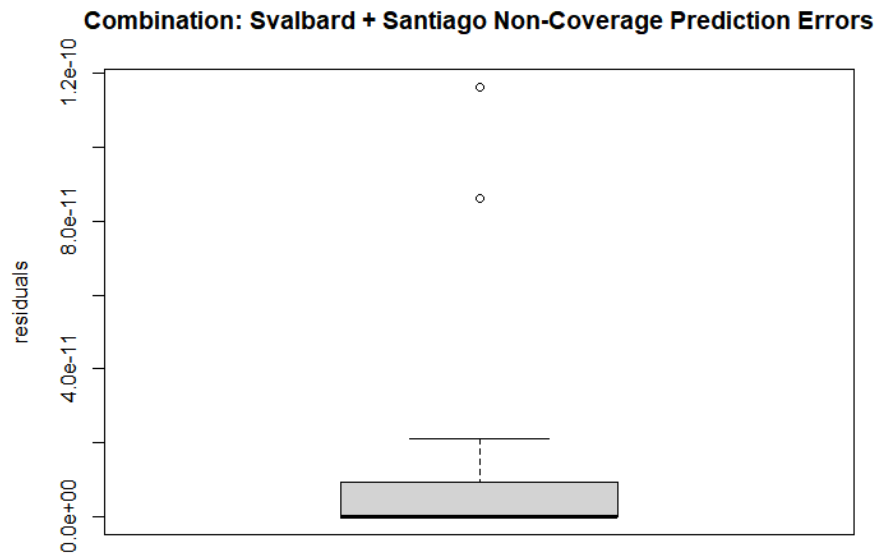


Figure 0-14. Distribution of errors between regression prediction values and simulation provided dataset at dataset values equal to 0.

DTE Combination: Svalbard + Santiago + Panama Coverage Results

A second round of combination of location datasets was selected to demonstrate the non-ZIP model application as well as the general regression form's application to an even higher degree of combinations. Svalbard and Santiago were selected; partly due to the familiarity of their pooled dataset from the previous section, and partly because their combination with Panama results in a somewhat evenly distributed spacing across latitude that is not likely to resulting in non-coverage values at any inclination. This absence of non-coverage values is also important to demonstrate due to the assumption that as additional locations are added to the combination pool, the less likely any particular user orbit is to not see coverage, and such a

scenario would speak to the robustness of the modeling practice intended for any possible combination of locations. **Figure 0-15** below shows the non-ZIP model overlayed with the simulation provided datapoints.

Combination: Svalbard + Santiago + Panama Coverage Regression

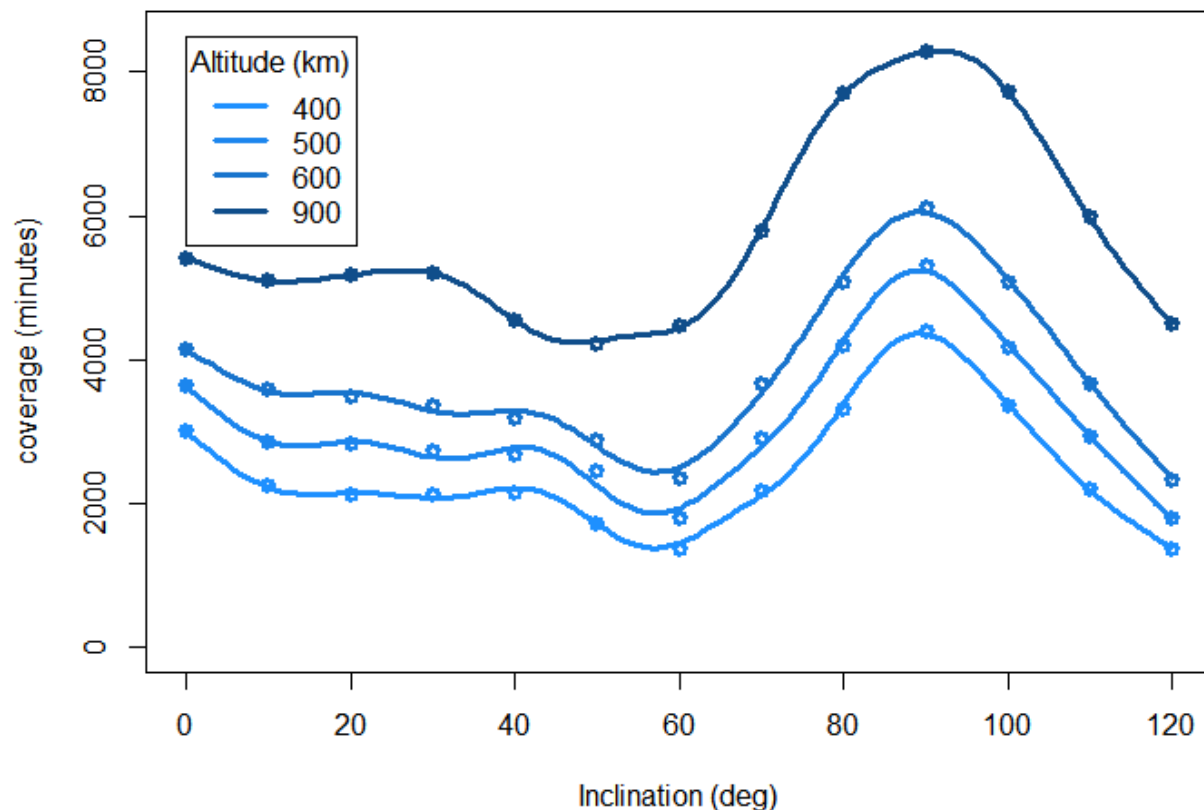


Figure 0-15. GAM regression for visibility-based coverage for a summation of generic Svalbard, Santiago, and Panama based ground station location coverages over 30 days.

Figure 0-16 below shows the literal errors between the regression predictions and summation of simulation provided datapoints. Note the significant reduction in range of errors compared to the previous ZIP models despite similar, or even greater range in predicted values.

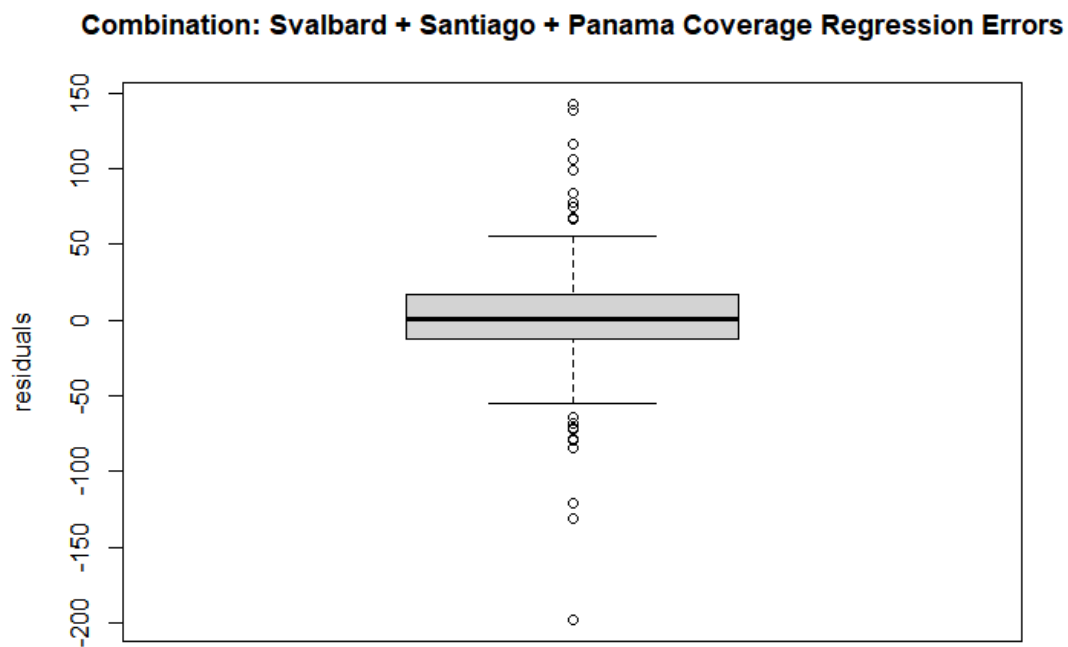


Figure 0-16. Distribution of errors between regression prediction values and simulation provided dataset.